633-5

(1)

(14) TG-446
May 1963
Copy No. 34

ANALYTICAL APPROXIMATIONS FOR STATIONARY CONICAL DETONATIONS AND DEFLAGRATIONS IN SUPERSONIC FLOW

by

Henry W. Woolard

THE JOHNS HOPKINS UNIVERSITY
APPLIED PHYSICS LABORATORY
8621 Georgia Avenue
SILVER SPRING MARYLAND

Operating under Contract NOw 62-0604-c with the Bureau of Naval Weapons, Department of the Navy

$ 7.60

The Johns Hopkins University
APPLIED PHYSICS LABORATORY
Silver Spring, Maryland

405038

SUMMARY

Approximate analytical relations are developed for several possible "conical" flow fields resulting from the steady supersonic flow of a uniform, non-viscous, non-heat conducting, combustible-gas mixture past a semi-infinite cone (at zero angle of attack) for instantaneous chemical reaction. The flow fields considered are of the shock-deflagration, detonation, and detonation-shock types with attached adiabatic and diabatic discontinuities. Particular emphasis is placed upon the Chapman-Jouguet detonation.

Parametric curves are presented for shock-deflagration flows about cones and wedges, and Chapman-Jouguet detonative flows about cones.

Generalized analyses of the flow characteristics of an oblique exothermic discontinuity are given in the appendices.

SYMBOLS

a	local speed of sound
a^*	normalized local speed of sound, a/c
c	maximum speed obtainable by adiabatically expanding into a vacuum (constant for any given region 0,1,2, etc.) $c = \sqrt{2\gamma R_T/(\gamma-1)}$
$C_3, C_4, --$	constants defined following Eq. (7)
C_γ, C_Q	functions defined respectively by Eqs. (B4) and (B6)
c_p	specific heat at constant pressure
c_v	specific heat at constant volume
k	$\cot \varphi_s$
k'	$\cot \varphi_a$
M	local Mach number, V/a
m	component of local Mach number normal to a conical ray, v/a (see Fig. 2)
p	static pressure
P	total pressure
Q	mechanical equivalent of heat added per unit mass of fluid (ft-lb/slug, or other consistent units)
Q/c_pT	heat-addition parameter (Damkohler's second parameter)

SYMBOLS (cont'd)

R	gas constant
T	static temperature
u,v	velocity components parallel and perpendicular respectively to a conical ray (see Fig. 2)
u^*,v^*	normalized velocity components, u/c, v/c
V	local resultant velocity, $\sqrt{u^2 + v^2}$
V_o	free-stream velocity
Γ	$(\gamma - 1)/2$
γ	ratio of specific heats, c_p/c_v
θ	local flow inclination relative to free-stream direction (see Fig. 2)
ρ	mass density
τ	total temperature
φ	spherical or polar angle (see Fig. 2)
$\varphi_{B_{max}}$	the maximum body semi-apex angle for which a conical flow region can exist for a given free-stream Mach number and heat release
φ_B^*	body semi-apex angle corresponding to a surface Mach number of unity
Ω_1,Ω_2,etc.	functions of γ defined in Appendix C

Subscripts

0,1,2,etc.	denotes a constant-value quantity in the particular region (see Fig. 1) indicated by the subscript
B	denotes conditions at the body surface
D	denotes conditions at a detonation wave
d	denotes conditions at any general exothermic discontinuity
F	denotes conditions at a deflagration wave
J	denotes conditions at, or pertaining to, a Chapman-Jouguet detonation
s	denotes conditions at a singular discontinuity
S	denotes conditions at an adiabatic shock wave
T	denotes juncture point of inner and outer solutions for the unit field
$(\pm)$	see statement following Eq. (B1b)
$[\pm]$	see statement following Eq. (B6)

Superscripts

$\sim$	indicates a variable quantity in region 0 (see Fig. 1)
—	indicates a variable quantity in region 1 (see Fig. 1)

Superscripts (cont'd)

$\overline{\overline{=}}$	indicates a variable quantity in region 2 (see Fig. 1)
(J)	denotes conditions corresponding to a Chapman-Jouguet detonation
(o)	see statement preceeding Eq. (B9)

INTRODUCTION

Although supersonic combustion in the form of a non-stationary Chapman-Jouguet detonation propagating through a tube filled with a combustible gas has been studied by combustion scientists for about eighty years (Refs. 1 and 2), it is only in recent times that experimental investigations have been conducted on supersonic combustion processes which are stationary with respect to an aerodynamic body, a fuel injection nozzle, or an exhaust nozzle (see, for example, Refs. 3 through 8). The motivation for the increased research activity in supersonic combustion stems from recent analyses of hypersonic ramjets utilizing supersonic combustions (Refs. 9, 10, and 11), proposals for detonative propulsion engines (Refs. 12 and 13), and studies of unconventional supersonic aircraft utilizing external burning for lift and for propulsion (Refs. 14 and 15). Hence, there are now practical as well as fundamental reasons for obtaining a more complete understanding of supersonic combustion processes.

It is observed, with regard to the detonative supersonic combustion experiments of Refs. 4, 5, and 6 that blunt bodies are more conducive to initiating shock-induced combustion than pointed ones because of the relatively higher

static temperature behind the normal shock. On the other hand, it seems only logical that greater dividends are derived from experimental investigations performed on configurations amenable to analytical calculation. A wedge is much more satisfactory in this respect than a blunt body. A cone, however, is not only amenable to analytical calculation (at least for the idealized case of instantaneous chemical reaction) but also represents a configuration which is adaptable either to the technique of firing in a gas-filled ballistic range or to stationary testing in a combustion wind tunnel. This overlapping of available testing techniques can hardly fail to be rewarding. Also, a cone is free of the end effects encountered on a finite-span wedge. A wedge has the advantage, however, of producing a stronger shock than a cone for a given apex angle and free-stream Mach number. Experimentally this can be compensated for in cone tests by increasing the temperature of the ambient gas in the tunnel or range.

This paper presents approximate analytical relations for several possible "conical" flow fields resulting from the steady supersonic flow of a uniform, non-viscous, non-heat conducting, combustible-gas mixture past a semi-infinite cone (at zero angle of attack) for instantaneous chemical reaction. Aside from its fundamental aspects, the

primary purpose of the paper is to present material which it is hoped will be useful in the design and interpretation of cone-flow supersonic combustion experiments aimed at obtaining a better understanding of the basic phenomena involved in supersonic combustion.

It appears that the only other theoretical work dealing with non-linear diabatic cone-flow fields is that of Kvashnina and Chernyi (Ref. 16). Kvashnina and Chernyi, without recourse to numerical calculation, deduce from an examination of the hodograph differential equation, the detonation hodograph, and the cone boundary condition, the general character of the flow field for the flow of a supersonic gas stream past a solid cone with an attached detonation wave and varying amounts of heat release.

Although supersonic combustion flow about a cone is the main topic of this paper, some numerical results for wedge combustion flow fields are included as a matter of interest.

GENERAL DESCRIPTION OF SOME POSSIBLE CONICAL FLOW REGIMES FOR INSTANTANEOUS CHEMICAL REACTION

The assumption of instantaneous chemical reaction allows a combustion zone (detonation or deflagration) to be treated as an exothermic surface of infinitesmal thickness

across which the flow properties and chemical compositions are discontinuous. An illustration showing some possible theoretical supersonic conical flow fields with an exothermic discontinuity appears in Fig. 1. The detailed notation, applied to a particular case of Fig. 1, is illustrated in Fig. 2. The adiabatic shocks appearing in Fig. 1 are assumed not to produce a change in the specific heats or in chemical composition. The different chemical compositions in the regions upstream and downstream of an exothermic discontinuity are frozen throughout their respective fields and the gas is assumed to be calorically and thermally perfect throughout a given region although it experiences an instantaneous change in the specific heats in crossing an exothermic discontinuity. The bounded flow fields between discontinuities (shocks, deflagrations, detonations, and bodies) are conical in the sense that the flow properties are constant along straight line elements emanating from the apex of the body. This is representative of the flow field for a chemically reacting mixture with finite reaction time in the region far away from the apex. In the vicinity of the apex, for distances of the order of the chemical relaxation distance, the flow will not be conical. The reduction of the flow problem to one involving conical fields represents a considerable simplification in the analytical task.

For an ambient stream of a given chemical composition the consequences of the chemical reactions are implicitly included in the aerothermodynamic parameters of the oblique exothermic discontinuity relations given in Appendix A. Since it is beyond the scope of this paper to treat the thermochemical aspects of the flow in detail, those quantities which would be determinate if the governing thermochemical relations were included are assumed to be known "a priori". These include, the heat release, the specific heats downstream, and the normal-component Mach number upstream of the exothermic discontinuity.

The oblique exothermic discontinuities shown in Fig. 1 are classified by applying Jouguet's rule (Ref. 17) for one-dimensional reactive flow to the normal components of the upstream and downstream Mach numbers at the discontinuity. Hence, immediately ahead of an oblique exothermic discontinuity the normal Mach-number component relative to the discontinuity is subsonic for a deflagration and supersonic for a detonation. The downstream normal Mach-number component is subsonic for a weak deflagration or a strong detonation, and supersonic for a strong deflagration or a weak detonation. Oblique Chapman-Jouguet deflagrations and detonations are those for which the downstream normal Mach-number component is unity.

The use of the adjectives "strong" and "weak" in the foregoing classification leads to an ambiguity in terminology if the traditional method of describing an oblique adiabatic shock due to a cone or wedge as strong or weak in accordance with the magnitude of its inclination angle is carried over to the diabatic shock case, since, in a manner analogous to adiabatic flow, two detonation-wave angles are obtained for a cone or wedge at a given free-stream Mach number, and a given detonative-wave heat release. The ambiguity[1] is avoided by designating the detonation wave with the larger inclination as "strongly inclined" and the one with the lesser inclination as "weakly inclined". Hence, an oblique strong detonation may be a weakly-inclined strong detonation or a strongly-inclined strong detonation. Similar descriptions are applied to weak detonations and to C-J detonations.

It can be shown from entropy considerations (Ref. 17) that strong deflagrations are impossible. For one-dimensional detonations, the literature is controversial (Refs. 1 and 2) regarding the theoretical existence of non C-J detonations, although the preponderant opinion seems

---

[1]This situation does not occur for oblique adiabatic shocks with constant specific heats, since consideration is never given to classifying such shocks in terms of their normal-flow properties because the normal-flow weak solution yields the result that "nothing happens" see Eq. (A6).

to be that Chapman-Jouguet detonations are the most probable, and that strong detonations are more probable than weak ones. For plane (wedge) flow, Siestrunch and associates (Ref. 18) have theoretically demonstrated the impossibility of weak detonations from an examination of the detonation polar without recourse to entropy considerations. For cylindrical (cone) flow Kvashnina and Chernyi (Ref. 16) imply the non-existence of weak detonations. In any case, the present analysis is generally confined to weak deflagrations, strong detonations, and Chapman-Jouguet detonations all having weak inclination angles. The restriction to weak inclinations follows by analogy to oblique adiabatic shocks for which only weak inclinations are observed in physical reality.

For plane flow, the shock-deflagration and the detonation flow regimes shown in Fig. 1 have been analyzed previously in Refs. 19 and 20, and Refs. 16, 21, and 22 respectively. A relatively superficial examination of the problem is sufficient to convince one's self that there also exist cylindrical flows having the same general character, although the field details differ in that for cylindrical flows, the pressure increases in the downstream direction along curved streamlines in bounded conical-flow regions, whereas for plane flows the pressure is constant on straight streamlines in bounded conical-flow regions.

For the detonative type flows it is pertinent to note that there are two particular values of the body semi-apex angle φ_B (for both cones and wedges) which are crucial to the delineation of the detonative-flow regimes shown in Fig. 1. For given values of the free-stream Mach number, specific heats, and heat release at the detonation wave, there exists a maximum body semi-apex angle $\varphi_{B_{max}}$ above which a conical flow (plane or cylindrical) cannot exist, i.e., the wave becomes detached, and there exists also a semi-apex angle φ_{B_J}, $\varphi_{B_{max}} \geq \varphi_{B_J}$, at which the detonation wave becomes a Chapman-Jouguet detonation. For body semi-apex angles less than $\varphi_{B_{max}}$ but greater than φ_{B_J} the flow equations yield two solutions, as previously noted, one of which corresponds to a strongly-inclined detonation wave and the other to a weakly-inclined detonation wave. For body semi-apex angles less than φ_{B_J}, the detonative wave angle remains at φ_J, and an expansion region occurs downstream of the detonation wave. This expansion region has a different character for plane and cylindrical flows. For plane flow, the expansion region is simply a Prandtl-Meyer expansion of sufficient extent to turn the flow parallel to the body surface. For cylindrical flow, Kvashnina and Chernyi in Ref. 16 ascertain that the conical expansion field adjacent

to the detonation wave is bounded on the downstream side by a shock wave followed by a compression flow field between the shock and cone (Fig. 1d). As the cone angle decreases, the width of the expansion zone increases, while the intensity of the shock wave at first increases and then begins to decrease until it degenerates into a characteristic. The flow direction on this characteristic is parallel to the axis of symmetry. An isentropic compression then occurs between the characteristic and the cone surface. When the cone angle is decreased still further the amount of compression is reduced until at zero cone angle it disappears entirely and the region behind the conical expansion region is uniform and parallel to the axis of symmetry.

For a cone, the detonative flow in Fig. 1c bears a close relationship to the adiabatic flow of Fig. 1a as now will be demonstrated.

If, in an adiabatic flow with a given cone angle, normalized cone-surface velocity u_B^*, and specific heat ratio, the normalized governing differential equation (see Eq. (1)) is integrated forward of the cone, ignoring the upstream boundary condition, an upper bound to the extent of the conical-flow field is found to occur at the singular

discontinuity[1] surface, φ_s, shown in Fig. 1a (Ref. 25). This singular behavior in the differential equation occurs at $v = a$, which is identical to the Chapman-Jouguet condition for diabatic flow. Therefore, when the detonation in Fig. 1c is a C-J detonation ($\varphi_D = \varphi_J$), the flows in the bounded regions ($\varphi_s \geq \varphi \geq \varphi_B$) and ($\varphi_J \geq \varphi \geq \varphi_B$) of Figs. 1a and 1c respectively are identical for a specified cone angle, normalized cone-surface velocity, and specific heat ratio. It is well known (Ref. 23) that for adiabatic cone flow there exists no uniform upstream flow that can be matched to the conical flow region bounded by the solid cone and the singular discontinuity surface. However, for a diabatic flow with known values of the specific heats on both sides of the exothermic discontinuity, it is possible, for cone angles less than $\varphi_{B_{max}}$, to find a uniform upstream flow having a Mach number and total temperature compatible with the existence of a Chapman-Jouguet exothermic discontinuity at the singular surface. Furthermore for any assumed wave angle φ_D, less than φ_J but greater than φ_s, it is possible to match that portion of the foregoing conical region

---

[1] Also called the "limit line" (Ref. 23) or "limit cone" (Ref. 24). Ref. 25 calls this discontinuity an "outer" discontinuity, since there exists also an "inner" discontinuity in the interior of the cone. This distinction will not be made herein since the "inner" discontinuity is not pertinent to the present problem.

bounded by φ_D and φ_B to a uniform free stream having a Mach number and total temperature compatible with an oblique detonation of inclination φ_D.

In view of the significant role played by the conical field bounded by a singular discontinuity and a solid cone it is convenient to refer to such a field as a unit conical field, or unit field (since v/a varies from 0 to 1.0). A unit field is uniquely defined by specifying φ_B, u_B^*, and γ or φ_s, u_s^*, and γ.

One of the purposes of this paper is to derive approximate relations for the unit conical field from which the detonative flows of Fig. 1c can be obtained. This has been done by developing a solution valid in the region of the singular discontinuity and one valid in the region of the cone surface and joining the two together at an intermediate location. The solution valid near the singular discontinuity provides also the initial field just downstream of the C-J detonation in the detonation-shock flow shown in Fig. 1d.

The approach taken in obtaining the diabatic conical flow fields considered herein is as follows.

For the shock-deflagration case, the free-stream Mach number and the adiabatic shock angle are specified. The corresponding adiabatic flow downstream of the shock is

obtained using one of the several approximate methods available in the literature. The inclination of the deflagration is then taken such that the desired upstream normal Mach number component is obtained ahead of the deflagration. For a given heat release the flow field downstream of the deflagration and the corresponding wedge or cone angle is then determined by the approximate method given herein in the next section.

For the detonation case, the free-stream Mach number, all the specific heats, and the C-J detonation wave angle are specified. The corresponding cone angle is then determined by the approximate method given herein. That portion of the unit field bounded by the C-J wave angle and the adiabatic shock angle then may be used to determine the upstream Mach number and total temperature corresponding to various strong detonation wave angles for fixed values of the cone angle, normalized cone-surface velocity, and unit-field specific heat ratio.

To the best of the writer's knowledge the case of a strong detonation on a wedge (Fig. 1c) is the only one of the reactive cases shown in Fig. 1 to have been observed experimentally (Ref. 6). An isolated attempt in Ref. 4 to produce a detonative reaction on a cone was unsuccessful.

It is not known whether the deflagration case shown in Fig. 1b can be produced in the laboratory. Aside from the uncertainties of ignition[1] and burning, the fluid dynamic aspects of the flow are somewhat restrictive with regard to laboratory experiments. As will be seen later, for plausible flame speeds and heat releases, the conical flow downstream of the deflagration is partially subsonic[2] for a fairly wide range of free-stream Mach numbers and cone angles. Such a flow, although theoretically acceptable for a semi-infinite body, cannot be attained in the laboratory because of practical considerations limiting the test model to a finite length. The existence of a subsonic region on a finite-length conical model results in the destruction of the conical flow as a consequence of the upstream propagation of downstream disturbances.

Assuming that a shock-deflagration flow (completely supersonic conical field) could be experimentally established, it presumably could be used to study (in a wind tunnel, say) the transition from deflagration to detonation by systematic

---

[1] An ignition system is necessary.

[2] Partially subsonic conical-flow regions exist also for the detonation and detonation-shock cases. In the detonation case (which is the one of principal interest here), however, the part of the flow spectrum for which this occurs is extremely small (see Fig. 13) for weakly-inclined detonations.

variations in the free-stream composition and aerothermodynamic conditions.

ANALYSIS

GOVERNING DIFFERENTIAL EQUATION

The governing differential equation for non-linear conical flow, normalized with respect to the maximum speed, c, is (Ref. 25),

$$\left(v^{*2} - a^{*2}\right)\left(d^2 u^*/d\varphi^2\right) = a^{*2}\left(2 u^* - v^* \cot \varphi\right) - u^* v^{*2} \tag{1}$$

where

$$v^* = - du^*/d\varphi \tag{2}$$

and

$$a^{*2} = \Gamma\left(1 - u^{*2} - v^{*2}\right) \tag{3}$$

THE UNIT CONICAL FLOW FIELD

The Outer Solution

If it is assumed that the right hand side of Eq. (1) is not zero at $\varphi = \varphi_s$, an expansion for u^* which will account for the singular behavior[1] and the boundary condition at φ_s is

$$u^* = u_s^* + a_s^* Z^2 + C_3 Z^3 + C_4 Z^4 + C_5 Z^5 + C_6 Z^6 + \text{---} \tag{4}$$

---

[1] Terms to be at least order of Z^3 in u^* must be retained to include the singular behavior.

from which

$$v^* = a_s^* + \frac{3}{2} C_3 Z + 2 C_4 Z^2 + \frac{5}{2} C_5 Z^3 + 3 C_6 Z^4 + \text{---} \qquad (5)$$

where

$$Z \equiv + (\varphi_s - \varphi)^{\frac{1}{2}}$$

and, from Eq. (3),

$$a_s^{*2} = \left(\frac{\gamma - 1}{\gamma + 1}\right)\left(1 - u_s^{*2}\right) \qquad (6)$$

with

$$+ (\varphi_s - \varphi)^{\frac{1}{2}} \ll 1.0 \qquad (7)$$

Substituting Eqs. (4) and (5) in Eq. (1), following some long and tedious algebraic manipulations, the relations for the coefficients in Eq. (4) are found to be

$$C_3 = \pm \left[(u_s^* - k\, a_s^*)\, a_s^*\right]^{\frac{1}{2}} \Big/ \Omega_1$$

$$C_4 = \Omega_2\, u_s^* + \Omega_3\, k\, a_s^*$$

$$C_5 = \left(\Omega_4\, u_s^{*2} + \Omega_5\, k\, u_s^*\, a_s^* + \Omega_6\, k^2\, a_s^{*2}\right) \Big/ C_3$$

$$C_6 = \left[\left(\Omega_7\, u_s^{*2} + \Omega_8\, a_s^{*2}\right) u_s^* + \left(\Omega_9\, u_s^{*2} - \Omega_8\, a_s^{*2}\right) k\, a_s^* + \Omega_{10}\, k^{*2}\, u_s^*\, a_s^{*2} + \Omega_{11}\, k^3\, a_s^{*3}\right] \Big/ C_3^2$$

Relations for the omega parameters Ω_1, Ω_2, etc., which are functions of γ, are given in Appendix C. Numerical values are listed in Table I for γ = 1.2, 1.3, 1.4, and 1.405[1].

For a compression flow the minus sign is selected in the expression for C_3 whereas for an expanding flow the plus sign is chosen.

The Inner Solution

Since v is zero at the cone surface, a reasonable approximation in the vicinity of the cone is

$$(v^*/a^*) \ll 1.0 \tag{8}$$

Utilization of the approximation of Eq. (8) in Eq. (1) results in the simplification of the governing differential equation to

$$d^2 u^* \Big/ d\varphi^2 + \cot \varphi\, (du^* \Big/ d\varphi) + 2\, u^* = 0 \tag{9}$$

---

[1]Value used in Ref. 25.

When Eq. (9) is expressed in terms of cos φ as an independent variable, it may be recognized as Legendre's differential equation of degree one.

The general solution to Eq. (9) is

$$u^* = A \cos \varphi + (B/2) \cos \varphi \log \left(\frac{1 + \cos \varphi}{1 - \cos \varphi} \right) - B \tag{10}$$

from which

$$v^* = A \sin \varphi + (B/2) \sin \varphi \log \left(\frac{1 + \cos \varphi}{1 - \cos \varphi} \right) + B \cot \varphi \tag{11}$$

and the constants A and B are determined at the juncture of the inner and outer solutions.

Equation (9) is frequently used in the literature to obtain an approximate solution for an adiabatic flow about a cone in supersonic or hypersonic main stream.

Joining of the Outer and Inner Solutions

In view of the restrictions of Eqs. (7) and (8) it is appropriate to join the inner and outer solutions at

$$\left(v^*/a^* \right)_T = \left(\varphi_s - \varphi_T \right)^{\frac{1}{2}} \tag{12}$$

Substituting Eq. (12) in Eq. (5), there is obtained

$$\left(\varphi_s - \varphi_T\right)^{\frac{1}{2}} = a_s^* + \frac{3}{2} C_3 \left(\varphi_s - \varphi_T\right)^{\frac{1}{2}} + 2 C_4 \left(\varphi_s - \varphi_T\right) + \frac{5}{2} C_5 \left(\varphi_s - \varphi_T\right)^{\frac{3}{2}} + 3 C_6 \left(\varphi_s - \varphi_T\right)^2 + \cdots \qquad (13)$$

In general Eq. (13) must be solved for φ_T by trial and error. If terms containing powers of $(\varphi_s - \varphi_T)$ greater than unity are negligible an analytic solution is obtained.

Once φ_T is known, the coefficients A and B are found by equating Eqs. (4) and (10) and Eqs. (5) and (11) at $\varphi = \varphi_T$ and solving the resulting equations. This procedure yields

$$B = \sin \varphi_T \left[v^*(\varphi_T;\varphi_s,u_s^*) \cos \varphi_T - u^* (\varphi_T;\varphi_s,u_s^*) \sin \varphi_T \right] \qquad (14)$$

$$A = \frac{u^* (\varphi_T;\varphi_s,u_s^*) - B \left[(1/2) \cos \varphi_T \log \left(\frac{1 + \cos \varphi_T}{1 - \cos \varphi_T} \right) - 1 \right]}{\cos \varphi_T} \qquad (15)$$

where $u^* (\varphi_T; \varphi_s,u_s^*)$ and $v^* (\varphi_T; \varphi_s,u_s^*)$ are obtained from Eqs. (4) and (5).

From the condition $v_B^* = 0$, and Eq. (11), the relation for determining the cone angle is found to be

$$\frac{1}{2} \log \left(\frac{1 + \cos \varphi_B}{1 - \cos \varphi_B} \right) + \frac{\cot \varphi_B}{\sin \varphi_B} = -\left(\frac{A}{B}\right) \qquad (16)$$

Equation (16) must be solved by trial and error for the value of φ_B corresponding to a given value of (-A/B). The plot in Fig. 4 is convenient for ascertaining a first approximation to φ_B, from which a more accurate value may be obtained, if so desired, by trial and error.

COMPARISON OF APPROXIMATE AND "EXACT" UNIT CONICAL FLOW FIELDS

It is desirable, of course, to verify the accuracy of the approximate unit field solution by comparing it with an exact solution. Apparently the only exact calculations performed for the complete unit field are those reported in Ref. 25[1]. Unfortunately Ref. 25 records[2] φ_s without giving the corresponding values of u_s^* or v_s^* required for the present purpose[3]. Examination of Table VI in Ref. 25, however, reveals that $(\varphi_S - \varphi_s)$ is generally less than 0.2 radians for a wide range of parameters. This suggests that u^* can

---

[1] The investigators in Ref. 25 performed these calculations principally as a matter of mathematical interest since they considered the singular discontinuity to be without physical significance.

[2] See Table VI and Diagram No. 8 in Ref. 25.

[3] An inquiry to MIT regarding the possibility of obtaining the values of u_s^* or v_s^* yielded negative results.

be developed in a series expansion in powers of $(\varphi - \varphi_S)$ from which u_s^* can be determined from the known value of φ_s given in Ref. 25. The appropriate expressions for this purpose are derived in Appendix D. This procedure should give a reasonably good value for u_s^*. However, derivatives of u^* will be less accurate near φ_s as a consequence of the singular behavior at φ_s which is not accounted for in the series expansion. For this reason v_s^* is calculated from Eq. (3)[1] rather than from the derivative of the series for u^*.

Exact unit-field solutions also can be obtained by the more laborious process of extending the flow fields of Ref. 25 forward of the shock position by means of a numerical integration procedure. Using the Runge-Kutta integration technique, one such calculation has been performed as a check on the accuracy of the series expansion method. In order to provide a relatively severe test, an example was selected for which $(\varphi_s - \varphi_S)$ is moderately large. The parameters of the example are $\varphi_B = 40$ deg., $u_B^* = 0.40$, $\varphi_S = 59.431$ deg. and $\varphi_s = 68.555$ deg. (corresponding to the flow field on p. 429 of Ref. 25). Values of $\varphi_s = 68.556$ deg. and $u_s^* = 0.30969$ were obtained from the Runge-Kutta integration. The series expansion method gave a value of $u_s^* = 0.31050$ for the retention of terms in the series to

---

[1] Recalling that $a_s^* = v_s^*$.

order $(\varphi - \varphi_S)^2$, and a value of $u_s^* = 0.31017$ for retention of terms to order $(\varphi - \varphi_S)^3$. It can be seen from these comparisons that the series expansion method predicts u_s^* rather well. It can be anticipated that in general the agreement will be better than in the example for smaller values of $(\varphi_s - \varphi_S)$ and poorer for larger values.

"Exact" values of u_s^* used in subsequent comparisons are based on the retention of terms to the order of $(\varphi - \varphi_S)^2$ in the series expansion.

Approximate and exact calculations of the flow field for the foregoing example are shown in Fig. 5. In the approximate calculation the outer solution was calculated retaining terms to the order of $(\varphi_s - \varphi)^3$ in u^*. It is apparent that the approximate calculation agrees very well with the exact one.

The results of additional computations comparing exact and approximate values of the cone semi-apex angle and the normalized cone-surface velocity for given values of φ_s and u_s^* are recorded in Table II. Also given in the table are, the joining angle φ_T for the inner and outer solutions, and the free-stream Mach number M_{o_J} for which the unit field corresponds to a Chapman-Jouguet detonation[1]. Note that the

[1]The free-stream Mach number, M_{o_J}, is found by substituting the C-J condition in Eq. (29) and solving the resulting quadratic equation in $M_{o_J}^2$.

cone-angle error $(\varphi_B - \varphi_B')/\varphi_B'$ generally increases with increasing values of $(\varphi_s - \varphi_B')/\varphi_s$, and that the error is generally larger for the smallest cone angle. Note also, that for a given cone angle, the cone-angle error decreases with increasing free-stream Chapman-Jouguet Mach number. The error in the cone-surface velocity is seen to be very small.

The cone-angle error is within acceptable limits for the 30- and 40-degree cones and the 10-degree cone at C-J Mach numbers greater than 3.0, but is, perhaps, of marginal acceptability for the 10-degree cone at C-J Mach numbers of less than 3.0.

The larger cone angles are of greater interest for detonation experiments since their stronger shocks are more conducive to producing a detonation.

Approximate and exact calculations of the flow field for Example VI in Table II are shown in Fig. 6.

THE DETONATION FLOW FIELD

The flow field under consideration is shown in Fig. 1c, with the subscript "0" denoting free-stream conditions and the subscript "2" denoting conditions in the field between the exothermic discontinuity and the cone.

As previously noted, it is assumed that M_o, c_{p_o}, c_{v_o}, c_{p_2}, c_{v_2}, and φ_J are known.

Consider first the determination of the tangential velocity component downstream of the Chapman-Jouguet wave. From the condition of constancy of the tangential velocity component across the wave there is obtained the relation

$$\bar{u}_J^* = M_o \, (\cos \varphi_J)(a_o/c_2)_J \tag{17}$$

where $(a_o/c_2)_J$ may be shown to be given by

$$\left[\left(\frac{a_o}{c_2}\right)_J = \left(\frac{\gamma_2 - 1}{2}\right)\left(\frac{\gamma_o R_o}{\gamma_2 R_2}\right)\left(\frac{\tau_o}{\tau_2}\right)_J \left(\frac{T}{\tau}\right)_o\right]^{\frac{1}{2}} \tag{18}$$

with $(\tau_o/\tau_2)_J$ obtained from Eq. (A16) as

$$\left(\frac{\tau_o}{\tau_2}\right)_J = \left(\frac{c_{p_o}}{c_{p_2}}\right)\left[1 + \left(\frac{Q}{c_{p_o} T_o}\right)_J \left(\frac{T}{\tau}\right)_o\right] \tag{19}$$

where, from Eq. (B3)

$$\left(\frac{Q}{c_{p_o} T_o}\right)_J = \frac{1}{2}\left(\frac{\gamma_o - 1}{\gamma_2^2 - 1}\right)\left[M_o^2 \sin^2 \varphi_J - 2\left(\frac{\gamma_2^2 - 1}{\gamma_o - 1} - \frac{\gamma_2^2}{\gamma_o}\right) + \left(\frac{\gamma_2}{\gamma_o}\right)^2 \frac{1}{M_o^2 \sin^2 \varphi_J}\right] \tag{20}$$

and

$$(T/\tau)_o = 1 + \left(\frac{\gamma_o - 1}{2} M_o^2\right)^{-1} \tag{21}$$

With $\bar{\bar{u}}_J^*$ and φ_J known, φ_B and $\bar{\bar{u}}_B^*$ may be determined by means of the unit field solution.

By manipulating Eq. (3), which is valid throughout field 2, the surface Mach number is easily shown to be given by

$$\bar{M}_B^2 = \frac{2}{\gamma_2 - 1} \bar{\bar{u}}_B^{*2} \left(1 - \bar{\bar{u}}_B^{*2}\right)^{-1} \tag{22}$$

The corresponding surface pressure is

$$\frac{\bar{p}_B}{p_o} = \frac{1}{(p/P)_o} \left(\frac{\bar{P}}{P_o}\right)_J \left(1 + \frac{\gamma_2 - 1}{2} \bar{M}_B^2\right)^{\frac{-\gamma}{\gamma - 1}} \tag{23}$$

where $(p/P)_o$ is given by Eq. (A19) with M_o replacing M, and $(\bar{P}/P_o)_J$ is obtained by specializing Eq. (A17) to the C-J condition and replacing $\bar{P}$ and $\bar{p}$ by P_o and p_o respectively.

From the aforementioned unit-field solution, values of $\bar{\bar{u}}_D^*$ and $\bar{\bar{v}}_D^*$ corresponding to an arbitrarily assumed value of φ_D are readily found. The corresponding values of M_o and $(Q/c_{p_o} T_o)$ are then determined as follows. From the condition of constancy of the tangential velocity component across the

detonation wave, and from relations for a non-Chapman-Jouguet detonation analogous to those of Eqs. (18), (19) and (20), it may be shown that

$$\Gamma_o \, M_o^2 \sin^2 \varphi_D \left[\left(\frac{\bar{u}}{c_2} \right)_D^2 \csc^2 \varphi_D - \cot^2 \varphi_D \right] + \left(\frac{\bar{u}}{c_2} \right)^2 \left[\left(\frac{Q}{c_{p_o} T_o} \right) + 1 \right] = 0 \tag{24}$$

where, from Eq. (A5)

$$\left(Q / c_{p_o} T_o \right) = f_1 \, \Gamma_o \, M_o^2 \sin^2 \varphi_D + f_2 - 1 \tag{25}$$

with

$$f_1 = \frac{2}{(\gamma_2 - 1)} \left[- \frac{(\gamma_2 + 1)}{2} \left(\frac{\bar{v}}{\tilde{v}} \right)_D^2 + \gamma_2 \left(\frac{\bar{v}}{\tilde{v}} \right)_D - \frac{(\gamma_2 - 1)}{2} \right] \tag{26}$$

$$f_2 = \frac{\gamma_2}{\gamma_o} \left(\frac{\gamma_o - 1}{\gamma_2 - 1} \right) \left(\frac{\bar{v}}{\tilde{v}} \right)_D \tag{27}$$

and

$$\left(\frac{\bar{v}}{\tilde{v}} \right)_D = \cot \varphi_D \left(\frac{\bar{v}/c_2}{\bar{u}/c_2} \right) \tag{28}$$

Solving Eqs. (24) and (25) for M_o^2, there is obtained

$$M_o^2 = f_2 \left[\Gamma_o \sin^2 \varphi_D \left(\frac{\cot^2 \varphi_D}{(\bar{u}/c_2)^2} - \csc^2 \varphi_D - f_1 \right) \right]^{-1} \tag{29}$$

The corresponding heat release is found by substituting Eq. (29) in Eq. (25). Obviously φ_D must be restricted to $\varphi_J \geq \varphi_D \geq \varphi_S$.

The surface Mach number as given by Eq. (22) is unchanged. The surface pressure is

$$\frac{\bar{p}_B}{p_o} = \frac{1}{(p/P)_o} \left(\frac{\bar{P}}{P_o} \right)_D \left(1 + \frac{\gamma_2 - 1}{2} \bar{M}_B^2 \right)^{\frac{-\gamma_2}{\gamma_2 - 1}} \tag{30}$$

Where $(p/P)_o$ is given by Eq. (A19) with M_o replacing M, and $(\bar{P}/P_o)_D$ is given by Eq. (A17) applied to a detonation, with P_o and p_o replacing $\bar{P}$ and $\bar{p}$.

The error in the approximate detonation field calculation is, of course, of the same order as the unit-field approximation upon which it is based.

THE DETONATION-SHOCK FLOW FIELD

It is not the purpose here to treat this flow field (Fig. 1d) in any detail. The initial portion of the expanding flow downstream of the Chapman-Jouguet wave may be obtained by

selecting the plus sign in the expression for C_3 in the outer solution of the unit field.

THE SHOCK-DEFLAGRATION FLOW FIELD

The treatment of this field requires approximations for the adiabatic portion of the field, region 1 in Fig. 1b, and the diabatic portion, region 2 in Fig. 1b. There are a wide variety of approximations available in the literature (see, for example, Refs. 26 through 31) for adiabatic cone flow. It is worth noting that for most of these the accuracy of the approximation increases with increasing free-stream Mach number (see Ref. 30). The unit-field solution presented herein also may be used for calculation of the adiabatic field.

If the shock-deflagration flow is confined to situations in which the normal-component Mach number ahead of the flame is of the order of that occurring in turbulent and laminar flames (say ≤ 0.10) the diabatic portion of the field in Fig. 1b may be approximated by the Legendre-type solution used in the inner portion of the unit field.

For known velocity components just downstream of the deflagration, a Legendre-type solution for the region 2 in Fig. 1b yields

$$\bar{\bar{u}}^* = \bar{\bar{A}} \cos \varphi + (\bar{\bar{B}}/2) \cos \varphi \log \left(\frac{1 + \cos \varphi}{1 - \cos \varphi} \right) - \bar{\bar{B}} \qquad (31)$$

$$\bar{\bar{v}}^* = \bar{A} \sin \varphi + (\bar{B}/2) \sin \varphi \log\left(\frac{1 + \cos \varphi}{1 - \cos \varphi}\right) + \bar{B} \cot \varphi \tag{32}$$

where

$$\bar{B} = \sin \varphi_F \, (\bar{\bar{v}}_F^* \cos \varphi_F - \bar{\bar{u}}_F^* \sin \varphi_F) \tag{33}$$

$$\bar{A} = \frac{\bar{\bar{u}}_F^* - \bar{B}\left[(1/2) \cos \varphi_F \log\left(\frac{1 + \cos \varphi_F}{1 - \cos \varphi_F}\right) - 1\right]}{\cos \varphi_F} \tag{34}$$

The cone angle corresponding to a specified deflagration (hence, known values of $\bar{A}$ and $\bar{B}$) may be found by means of Eq. (16) with $\bar{A}$ and $\bar{B}$ replacing A and B.

The surface Mach number is given by Eq. (22). The corresponding surface pressure is

$$\frac{\bar{\bar{p}}_B}{p_o} = \frac{1}{(p/\bar{p})_o}\left(\frac{\bar{p}}{p_o}\right)_S \left(\frac{\bar{\bar{p}}}{\bar{p}}\right)_F \left(1 + \frac{\gamma_2 - 1}{2} \bar{\bar{M}}_B^2\right)^{\frac{-\gamma_2}{\gamma_2 - 1}} \tag{35}$$

where $(\bar{p}/p_o)_S$ is obtained from oblique shock relations (see e.g. Ref. 32), (p/p_o) is given by Eq. (A19) with M_o replacing M, and $(\bar{\bar{p}}/\bar{p})_F$ is given by Eq. (A17) applied to a deflagration.

SOME PARAMETRIC CURVES

A limited number of parametric curves of the properties of some supersonic flows with oblique discontinuities

are presented herein in Figs. 7 through 12. These curves are not intended to be comprehensive; such a goal is beyond the scope of this work. Nor are they intended to be the direct result of applying the foregoing approximations, since, where possible, existing tabulated fields are used in part. The purpose is simply one of illustrating some trends and magnitudes for parametric values within an approximate range of possible interest.

Figures 7 and 8 present curves which are plots of Eqs. (A5), (A8), (A12) and (A14), or combinations thereof. These curves, along with the remaining equations of the collection (A9) through (A19), permit the determination of the flow properties across oblique deflagrations for normal-component Mach numbers ranging in value from 0.0 to 0.10, at a constant specific heat ratio of 1.4

Some flow properties for the shock-deflagration regime illustrated in Fig. 1b are given in Figs. 9 and 10 for cone flows and in Figs. 11 and 12 for wedge flows for a constant specific heat ratio of 1.4, free-stream Mach numbers of 2.0, 4.0, and 6.0, flame normal-component Mach numbers of 0.040 and 0.80, and identical adiabatic shock angles for the cone and wedge cases.

Curves of the body semi-apex angle as a function of the normal-component velocity ratio across the flame, for constant values of specific heat ratio, free-stream Mach

number, shock angle, and flame normal-component Mach number are shown in Figs. 9 and 11 respectively for cones and wedges. The flame inclination angles are also indicated on the figures. Shown in Figs. 10 and 11 are the associated cone- and wedge-surface Mach numbers from which the surface pressure may be calculated by means of Eq. (35). The corresponding heat release parameter is ascertainable from Fig. 7.

The adiabatic portion of the cone shock-deflagration flow field required in the construction of the curves in Figs. 9 through 12 was obtained from the tables of Ref. 33. The flame inclination corresponding to a preassigned stream Mach number, shock-wave angle, and flame normal-component Mach number was found by interpolation in the table of Ref. 33. The cone angle corresponding to a given normal-component velocity ratio across the flame (Fig. 9) was then determined by means of a Legendre-type solution.

The construction of the wedge-flow curves in Figs. 11 and 12 involved a rather straight forward application of the oblique shock relations (Ref. 32) and the appropriate equations in Appendix A.

An important point worth noting with regard to Figs. 10 and 12 is the fairly large portion of the parametric spectrum for which the body-surface Mach number is subsonic.

This indicates that the conical flow downstream of the deflagration is partially subsonic for a fairly wide range of free-stream Mach numbers and cone angles. As previously noted, such a flow cannot be attained in the laboratory since on a finite-length model the conical flow is destroyed by the upstream propagation of downstream disturbances in the subsonic field. In experiments aimed at attaining a shock-deflagration type of flow, it is therefore necessary to constrain the parameters to values for which the flow is completely supersonic downstream of the deflagration. In this regard it is observed from Figs. 10 and 12 that the parametric spectrum for which the flow downstream of the deflagration is completely supersonic increases in range with increasing free-stream Mach number.

For cone flow, curves of the Chapman-Jouguet wave angle as a function of free-stream Mach number for various cone angles and a constant specific-heat ratio of 1.405 are shown in Fig. 13 along with the corresponding adiabatic shock-wave angles. The detonation curves were obtained by extending the flow fields given in Ref. 25 forward to the known singular discontinuity surface of Ref. 25 by means of the series expansion method described in the section "Comparison of Approximate and Exact Unit Conical Flow Fields." The previously described similarities in the characteristics of the detonation and adiabatic shock waves

are readily apparent in the figure. The condition for which sonic velocity occurs at the cone surface is indicated by the circular and triangular symbols respectively for detonation and adiabatic shock waves. The corresponding cone angles are $\varphi_{B_J}^*$ and $\varphi_{B_o}^*$. As noted on the figure, the surface Mach number is subsonic for detonation wave angles greater than the wave angle for a sonic surface velocity, and supersonic for lesser wave angles.

Since a sonic surface velocity is the limiting condition for the attainment of conical flow on a finite length model in an experimental facility, an "a priori" knowledge of $\varphi_{B_J}^*$ is important to the selection of a test model for which the semi-apex angle should be as large as possible to promote detonation without destroying the conical flow. The adiabatic cone angle $\varphi_{B_o}^*$ is not satisfactory for this purpose since it is generally larger than $\varphi_{B_J}^*$. Note on Fig. 13, for example, that $\varphi_{B_J}^* = 30$ degrees for a free-stream Mach number of 2.2, whereas the corresponding adiabatic-flow cone angle $\varphi_{B_o}^*$ at the same Mach number is found to be 39.1 degrees (Ref. 32).

It is well known for adiabatic cone flow that there exists an absolute maximum cone angle above which a conical flow region cannot exist regardless of the free-stream

Mach number. For a specific heat ratio of 1.405 the value of this maximum angle is known to be 57.6 degrees (Ref. 25). The analogous absolute maximum cone angle for a C-J detonation flow was found herein to be 35.8 ($\pm$ 0.2) degrees.

CONCLUDING REMARKS

Approximate relations have been developed for calculating cone flow fields of the shock-deflagration and detonation types with attached adiabatic and diabatic discontinuities.

The appropriateness of the Lengendre-type approximation used for the shock-deflagration flow has been demonstrated various places in the literature in applications to adiabatic cone flow. The appropriateness of the present approximate method for detonative flow fields has been verified herein where it is shown that the error decreases with increasing cone angle and increasing free-stream Chapman-Jouguet Mach number.

It is believed that the analytical relations of this paper will be useful in the design and interpretation of cone-flow supersonic combustion experiments since there are no flow field tables available for the specific-heat ratios and conditions likely to be encountered in experiment,

and hand numerical integration of the governing differential equation involves a greater effort than does the present method. The availability to the researcher of a digital computer, of course, circumvents the use of the present method. Such facilities are not always available, however, and in any event the present method serves as a useful complement to machine calculation as well as providing useful relations for the machine program in the vicinity of the singular discontinuity.

APPENDIX A

Single Oblique Exothermic Discontinuity

Consider the deflagration shown in Fig. 2 to be any general exothermic discontinuity (detonation or deflagration) separating two conical flow fields. In view of the assumption of a perfect gas in the separate regions, the following thermodynamic relations and definitions apply in a given region: $p = \rho RT$, $R = c_p - c_v$, $a^2 = \gamma RT = \gamma p/\rho$, and $\gamma = c_p/c_v$.

With reference to Fig. 2, the equations of conservation of mass, normal momentum, tangential momentum, and energy across the discontinuity (denoted by the subscript d) are respectively,

$$\bar{\rho}_d \, \bar{v}_d = \bar{\bar{\rho}}_d \, \bar{\bar{v}}_d \tag{A1}$$

$$\bar{p}_d + \bar{\rho}_d \, \bar{v}_d^2 = \bar{\bar{p}}_d + \bar{\bar{\rho}}_d \, \bar{\bar{v}}_d^2 \tag{A2}$$

$$\bar{u}_d = \bar{\bar{u}}_d \tag{A3}$$

$$\frac{1}{2} \bar{v}_d^2 + c_{p_1} \bar{T}_d + Q = \frac{1}{2} \bar{\bar{v}}_d^2 + c_{p_2} \bar{\bar{T}}_d \tag{A4}$$

The foregoing derived forms of the momentum and energy equations are obtained from the basic forms through the use of the conservation of mass relation in the basic momentum equations and the conservation of mass and tangential momentum in the basic energy equation.

The equation of state, the relations $\bar{m}_d = \bar{v}_d/\bar{a}_d$ and $c_p = \gamma R/(\gamma - 1)$ and Eqs. (A1), (A2) and (A4) may be combined to give

$$\frac{Q}{c_{p_1}\bar{T}_d} = \bar{m}_d^2\left(\frac{\gamma_1 - 1}{\gamma_2 - 1}\right)\left[-\frac{(\gamma_2 + 1)}{2}\left(\frac{\bar{v}}{\bar{v}}\right)_d^2 + \gamma_2\left(\frac{\bar{v}}{\bar{v}}\right)_d - \frac{1}{2}(\gamma_2 - 1)\right]$$

$$+ \frac{\gamma_2}{\gamma_1}\left(\frac{\gamma_1 - 1}{\gamma_2 - 1}\right)\left(\frac{\bar{v}}{\bar{v}}\right)_d - 1 \qquad \text{(A5)}$$

Equation (A5) may be solved for $(\bar{v}/\bar{v})_d$. The result is

$$\left(\frac{\bar{v}}{\bar{v}}\right)_d = \frac{\left(\frac{\gamma_2}{\gamma_1} + \gamma_2\,\bar{m}_d^2\right) \pm F^{\frac{1}{2}}}{(\gamma_2 + 1)\,\bar{m}_d^2} \qquad \text{(A6a)}$$

where

$$F = \left(\frac{\gamma_2}{\gamma_1} - \bar{m}_d^2\right)^2 - 2\left[\frac{(\gamma_2 - \gamma_1)(\gamma_2 + 1)}{\gamma_1(\gamma_1 - 1)}\right]\bar{m}_d^2$$

$$- 2\,\bar{m}_d^2\left(\frac{\gamma_2^2 - 1}{\gamma_1 - 1}\right)\left(\frac{Q}{c_{p_1}\bar{T}_d}\right) \qquad \text{(A6b)}$$

and

$$\bar{m}_d = \bar{M}_d \sin (\varphi_d - \bar{\theta}_d) \tag{A7}$$

Discussion of the consequences of the selection of a specific sign preceding the radical in Eq. (A6a) is relegated to Appendix B.

Equation (A3) and the velocity vector diagram, Fig. 2, yield the following result for the change in flow direction across the discontinuity

$$\tan (\varphi_d - \bar{\theta}_d)/\tan (\varphi_d - \bar{\theta}_d) = (\bar{v}/\bar{v})_d \tag{A8}$$

Equations (A6) and (A8) are the governing relations for an oblique diabatic discontinuity. For known values of $\bar{m}_d$, φ_d, $\bar{\theta}_d$, $Q/c_{p_1}\bar{T}_d$, γ_1, and γ_2 the foregoing equations may be solved for $(\bar{v}/\bar{v})_d$ and $\bar{\theta}_d$. In some problems, different combinations of these parameters may be specified.

The density, static-pressure, static-temperature, sonic speed, and normal Mach-number ratios across the discontinuity may be expressed in terms of $(\bar{v}/\bar{v})_d$. Relations for the preceding quantities, derivable from Eqs. (A1) and (A2) and the basic thermodynamic relations and definitions are

$$\left(\bar{\rho}/\bar{\bar{\rho}}\right)_d = \left(\bar{\bar{v}}/\bar{v}\right)_d \tag{A9}$$

$$\left(\bar{\bar{p}}/\bar{p}\right)_d = 1 - \gamma_1 \bar{m}_d^2 \left[\left(\bar{\bar{v}}/\bar{v}\right)_d - 1\right] \tag{A10}$$

$$\left(\bar{\bar{T}}/\bar{T}\right)_d = \left(R_1/R_2\right)\left(\bar{\bar{v}}/\bar{v}\right)_d\left(\bar{\bar{p}}/\bar{p}\right)_d \tag{A11}$$

$$\left(\bar{\bar{a}}/\bar{a}\right)_d = \left[\left(\gamma_2/\gamma_1\right)\left(\bar{\bar{v}}/\bar{v}\right)_d\left(\bar{\bar{p}}/\bar{p}\right)_d\right]^{\frac{1}{2}} \tag{A12}$$

$$\left(\bar{\bar{m}}/\bar{m}\right)_d = \left[\left(\gamma_1/\gamma_2\right)\left(\bar{\bar{v}}/\bar{v}\right)_d/\left(\bar{\bar{p}}/\bar{p}\right)_d\right]^{\frac{1}{2}} \tag{A13}$$

where $\left(\bar{\bar{p}}/\bar{p}\right)_d$ in Eqs. (A11), (A12), (A13), is given by Eq. (A10).

The resultant-velocity ratio, the resultant Mach-number ratio, the stagnation-temperature ratio, and the stagnation-pressure ratio depend upon vector quantities. Utilization of Fig. 2, Eqs. (A3) and (A4) and basic definitions yield

$$\left(\bar{\bar{V}}/\bar{V}\right)_d = \cos\left(\varphi_d - \bar{\theta}\right)_d / \cos\left(\varphi_d - \bar{\bar{\theta}}\right)_d \tag{A14}$$

$$\left(\bar{\bar{M}}/\bar{M}\right)_d = \left(\bar{\bar{V}}/\bar{V}\right)_d\left(\bar{a}/\bar{\bar{a}}\right)_d \tag{A15}$$

$$\left(\frac{\tau_2}{\tau_1}\right) = \frac{c_{p_1}}{c_{p_2}}\left[1 + \left(\frac{Q}{c_{p_1}\bar{T}}\right)_d\left(\frac{\bar{\bar{T}}}{\bar{T}}\right)_d\right] \tag{A16}$$

$$(\bar{\bar{P}}/\bar{P})_d = (\bar{\bar{p}}/\bar{p})_d \; (\bar{p}/\bar{P})_d/(\bar{\bar{p}}/\bar{\bar{P}})_d \tag{A17}$$

where

$$(T/\tau) = \left[1 + \frac{\gamma - 1}{2} M^2\right]^{-1} \tag{A18}$$

$$(p/P) = \left[1 + \frac{\gamma - 1}{2} M^2\right]^{\frac{-\gamma}{\gamma - 1}} \tag{A19}$$

yield the required quantities in Eqs. (A16) and (A17) by appropriate substitution of $\bar{M}_d$ and $\bar{\bar{M}}_d$ for M.

A wide variety of alternate forms of the preceding relations may be obtained by suitable manipulations.

For specified values of γ_1, γ_2, and $Q/c_{p_1}\bar{T}_d$, the flow quantity ratios given by Eqs. (A6) and Eqs. (A9) through (A13) are functions of the normal component of the upstream Mach number in a manner analogous to the same well-known property for an oblique shock wave (adiabatic discontinuity). The stagnation pressure ratio, however, does not follow this analogous behavior in the diabatic case.

Equations (A6), (A10), and (A13) are analyzed in Appendix B for the purposes of delineating the boundaries of the various normal-component flow regimes and classifying them according to Jouguet's rule.

APPENDIX B

Delineation of the Normal-Component Flow Regimes for an Oblique Exothermic Discontinuity

For the discussion in this appendix it is convenient to rewrite Eq. (A6), introducing a special notation, as follows

$$\left(\frac{\bar{v}}{\bar{v}}\right)_{d(\pm)} = \frac{\left(\frac{\gamma_2}{\gamma_1} + \gamma_2 \bar{m}_d^2\right) \pm F^{\frac{1}{2}}}{(\gamma_2 + 1)\,\bar{m}_d^2} \tag{B1a}$$

where

$$F = \left(\frac{\gamma_2}{\gamma_1} - \bar{m}_d^2\right)^2 - 2\left[\frac{(\gamma_2 - \gamma_1)(\gamma_2 + 1)}{\gamma_1\,(\gamma_1 - 1)}\right]\bar{m}_d^2 - 2\,\bar{m}_d^2\left(\frac{\gamma_2^2 - 1}{\gamma_1 - 1}\right)\left(\frac{Q}{c_{p_1}\bar{T}_d}\right) \tag{B1b}$$

and the sign of the quantity $(\pm)$ in the subscript of $(\bar{v}/\bar{v})_d$ is taken to agree with the sign selected ahead of the radical. Quantities which are functions of $(\bar{v}/\bar{v})_d$ also carry the same subscript notation.

From Eq. (B1) it is seen that $(\bar{v}/\bar{v})_d$ is double valued for given positive values of F and $\bar{m}_d$, that there are two possible real values of $\bar{m}_d$ corresponding to given positive values of F and $Q/c_{p_o}\bar{T}_d$, and there are no real solutions for

$F < 0$. It is apparent therefore that the factors crucial to the delineation of the various normal-component flow regimes by means of Eq. (B1) are the magnitude of the function F and the choice of sign preceding the radical.

For $F = 0$, Eq. (B1a) becomes

$$\left(\frac{\bar{\bar{v}}}{\bar{v}}\right)_J = \frac{(\gamma_2/\gamma_1)(1 + \gamma_1 \bar{m}_d^2)}{(\gamma_2 + 1)\,\bar{m}_d^2} \tag{B2}$$

Substitution of Eq. (B2) in Eqs. (A10) and (A13) results in $\bar{m}_d = 1.0$; the Chapman-Jouguet condition.

From the expression for the derivative of $(\bar{\bar{v}}/\bar{v})_d$ with respect to $\bar{M}_d$ it is easy to show that the C-J condition ($F = 0$) is a singular point of Eq. (B1) for a constant Q. It is also easy to show, by means of Eq. (A5), that the C-J condition corresponds to the maximum heat release for a given value of $(\bar{\bar{v}}/\bar{v})_d$.

The heat release corresponding to the Chapman-Jouguet condition is given by

$$\left(\frac{Q}{c_{p_1}\,\bar{T}}\right)_J = \frac{1}{2}\left(\frac{\gamma_1 - 1}{\gamma_2^2 - 1}\right)\left[\bar{m}_d^2 - 2\,C_\gamma + \left(\frac{\gamma_2}{\gamma_1}\right)^2 \frac{1}{\bar{m}_d^2}\right] \tag{B3}$$

where

$$C_\gamma \equiv \frac{\gamma_2}{\gamma_1} + \frac{(\gamma_2 - \gamma_1)(\gamma_2 + 1)}{\gamma_1\,(\gamma_1 - 1)} \tag{B4}$$

Or, alternatively, the normal Mach-number component yielding the Chapman-Jouguet condition for a given heat release is

$$\bar{m}^2_{J\left[\pm\right]} = (C_\gamma + C_Q) \pm \left[(C_\gamma + C_Q)^2 - (\gamma_2/\gamma_1)^2\right]^{\frac{1}{2}} \tag{B5}$$

where

$$C_Q = \left(\frac{\gamma_2^2 - 1}{\gamma_1 - 1}\right)\left(\frac{Q}{c_{p_1}\bar{T}_d}\right) \tag{B6}$$

and the sign of the quantity $\left[\pm\right]$ in the subscript of $\bar{m}_J$ is taken to agree with the sign used ahead of the radical. Quantities which are functions of $\bar{m}_J$ also carry the same subscript notation. Note that the parenthetical subscript notation $(\pm)$ pertains to Eq. (B1) and quantities derived therefrom, whereas the bracketed subscript notation $\left[\pm\right]$ pertains to Eq. (B5) and correspondingly derived quantities. The effect of sign selection in Eq. (B1) upon the normal component of the downstream Mach number is now examined. Since $(\bar{p}/\bar{p})_d$ is a positive quantity*, and $(\bar{v}/\bar{v})_{d(+)} \geq (\bar{v}/\bar{v})_{d(-)}$, it follows from Eq. (A10) that $(\bar{p}/\bar{p})_{d(+)} \leq (\bar{p}/\bar{p})_{d(-)}$. Eq. (A13) then yields $\bar{m}_{d\ (+)} \geq \bar{m}_{d(-)}$. Since the C-J condition is the boundary between the plus and minus solutions of Eq. (B1a) there is obtained

$$\bar{m}_{d(-)} \leq 1.0 \leq \bar{m}_{d(+)} \tag{B7}$$

*The ratio $(\bar{p}/\bar{p})_d$ is positive for $(\bar{v}/\bar{v})_d \leq \left(1 + \frac{1}{\gamma_1 \bar{m}_d^2}\right)$.

That is, selection of the minus (-) sign in Eq. (B1a) gives a subsonic normal component for the downstream Mach number, whereas selection of the plus (+) sign gives a supersonic normal component for the downstream Mach number.

Two pairs of curves given by Eq. (B1) for constant values of Q, say Q_I and Q_{II}, ($Q_{II} > Q_I$) are illustrated in Fig. 3 for $\gamma_1 > \gamma_2$. The locus of the C-J points given by Eq. (B2) is shown by the curve ABC. It is obvious (as noted on the figure) that regions above the C-J curve correspond to the selection of the plus (+) sign in Eq. (B1a) and the regions below the curve correspond to the selection of the minus (-) sign.

As previously noted there are no real solutions to Eq. (B1a) for $F < 0$. Applying the condition $F < 0$ to Eq. (B1b), the normal-component Mach number range for which there are no solutions to Eq. (B1a) for specified values of γ_1, γ_2, and $Q/c_{p_1} \bar{T}_d$ is found to be

$$\bar{m}^2_{J[-]} < \bar{m}^2_d < \bar{m}^2_{J[+]} \tag{B8}$$

where $\bar{m}_{J[-]}$ and $\bar{m}_{J[+]}$ are given by Eq. (B3). The $\bar{m}_{J[+]}$ conditions for $Q = Q_I$ and Q_{II} occur at the points J' and j' respectively in Fig. 3. The corresponding $\bar{m}_{J[-]}$ conditions occur at the points J and j in the figure.

From Eqs. (B7) and (B8) it is apparent that there exists a heat-release quantity $Q^{(0)}$ at and below which real solutions to Eq. (B1) are obtained for all real values of $\bar{m}_d$. This occurs when $\bar{m}_{J[-]} = \bar{m}_{J[+]}$, for which the term under the radical in Eq. (B5) becomes zero. The corresponding values $(Q/c_{p_1}\bar{T}_d)^{(0)}$, $\bar{m}_J^{(0)}$, and $(\bar{\bar{v}}/\bar{v})_J^{(0)}$ are easily shown to be

$$(Q/c_{p_1}\bar{T}_d)^{(0)} = (\gamma_1 - \gamma_2)/\gamma_1\ (\gamma_2 - 1) \tag{B9}$$

$$\bar{m}_J^{(0)} = (\gamma_2/\gamma_1)^{\frac{1}{2}} \tag{B10}$$

$$(\bar{\bar{v}}/\bar{v})_J^{(0)} = 1.0 \tag{B11}$$

The velocity ratio curves are given by

$$\left.\begin{aligned} \left(\frac{\bar{\bar{v}}}{\bar{v}}\right)_{d(+)}^{(0)} &= 1.0 \\ \left(\frac{\bar{\bar{v}}}{\bar{v}}\right)_{d(-)}^{(0)} &= \frac{2\,\gamma_2/\gamma_1 + (\gamma_2 - 1)\,\bar{m}_d^2}{(\gamma_2 + 1)\,\bar{m}_d^2} \end{aligned}\right\} \bar{m}_d \geq \bar{m}_J^{(0)} \tag{B12}$$

$$\left.\begin{aligned}\left(\frac{\bar{v}}{\bar{v}}\right)^{(0)}_{d(+)} &= \frac{2\,\gamma_2/\gamma_1 + (\gamma_2 - 1)\,\bar{m}_d^2}{(\gamma_2 + 1)\,\bar{m}_d^2} \\ \left(\frac{\bar{v}}{\bar{v}}\right)^{(0)}_{d(-)} &= 1.0\end{aligned}\right\} \quad \bar{m}_d \le \bar{m}_J^{(0)} \tag{B13}$$

Curves for $Q = Q^{(0)}$ are shown in Fig. 3. Point B in the figure corresponds to $\bar{m}_J^{(0)}$.

If the parameters γ_2/γ_1, C_γ, and C_Q are of order unity, the following asymptotic forms for Eq. (B1) are readily obtained.

$$\left[\left(\frac{\bar{v}}{\bar{v}}\right)_{d(+)}\right]_{\bar{m}_d \to 0} = \left(\frac{\gamma_2/\gamma_1}{\gamma_2 + 1}\right)\left[\frac{2}{\bar{m}_d^2} + \gamma_1 - \frac{(C_\gamma + C_Q)}{(\gamma_2/\gamma_1)^2}\right] \tag{B14}$$

$$\left[\left(\frac{\bar{v}}{\bar{v}}\right)_{d(-)}\right]_{\bar{m}_d \to 0} = \left(\frac{\gamma_2/\gamma_1}{\gamma_2 + 1}\right)\left[\gamma_1 + \frac{(C_\gamma + C_Q)}{(\gamma_2/\gamma_1)^2}\right] \tag{B15}$$

$$\left[\left(\frac{\bar{v}}{\bar{v}}\right)_{d(+)}\right]_{\bar{m}_d \to \infty} = 1.0 \tag{B16}$$

$$\left[\left(\frac{\bar{v}}{\bar{v}}\right)_{d(-)}\right]_{\bar{m}_d \to \infty} = \frac{\gamma_2 - 1}{\gamma_2 + 1} \tag{B17}$$

Finally, the limiting boundaries for the regimes of exothermic discontinuities are delineated by the adiabatic condition Q = 0. For the adiabatic condition, note from Eq. (B1) that F is always positive and greater than zero, providing $\gamma_1 > \gamma_2$. Therefore, for Q = 0 and $\gamma_1 > \gamma_2$, real solutions to Eq. (B1) are obtained for all real values of $\bar{m}_d$.

In Fig. 3 the endothermic regions are indicated by the hatched areas. The shaded areas delineate regions of weak deflagrations and detonations, while the unshaded areas represent strong deflagrations and detonations. The bounding adiabatic curves, Q = 0, are noted.

Although the material presented in this appendix is not new in its entirety, it does cover the subject in a slightly more generalized manner than heretofore.

APPENDIX C

The Omega Functions

$$\Omega_1 = \frac{3}{2}(1+\Gamma)^{\frac{1}{2}}$$

$$\Omega_2 = -(5)(1+2\Gamma)/F_1$$

$$\Omega_3 = -(1-4\Gamma)/F_1$$

$$\Omega_4 = (17-10\Gamma+8\Gamma^2)/F_2$$

$$\Omega_5 = (41+32\Gamma-16\Gamma^2)/F_2$$

$$\Omega_6 = (-58-22\Gamma+8\Gamma^2)/F_2$$

$$\Omega_7 = (-320-2{,}280\Gamma-240\Gamma^2+320\Gamma^3)/F_3$$

$$\Omega_8 = (-5{,}040-10{,}440\Gamma-5{,}400\Gamma^2)/F_3$$

$$\Omega_9 = (150+3{,}780\Gamma-8{,}640\Gamma^2-960\Gamma^3)/F_3$$

$$\Omega_{10} = (1{,}920-3{,}240\Gamma+18{,}000\Gamma^2+960\Gamma^3)/F_3$$

$$\Omega_{11} = (-1{,}750+1{,}740\Gamma-9{,}120\Gamma^2-320\Gamma^3)/F_3$$

where

$$\Gamma = (\gamma-1)/2 \qquad F_1 = 12(1+\Gamma)$$

$$F_2 = 270(1+\Gamma)^2 \qquad F_3 = 72{,}900(1+\Gamma)^3$$

APPENDIX D

Conical Flow Field in the Vicinity of an Arbitrary Non-Singular Conical Ray

Denote the angular position of an arbitrary non-singular conical ray by φ_a, then

$$u^* = u_a^* - v_a^* (\varphi - \varphi_a) + A_2 (\varphi - \varphi_a)^2 + A_3 (\varphi - \varphi_a)^3 + \text{---} \qquad \text{(D1)}$$

where $(\varphi - \varphi_a)$ is a small quantity. Substitution of (D1) in Eqs. (1) through (3) yields

$$A_2 = \frac{2 u_a^* a_a^{*2} - k' v_a^* a_a^{*2} - u_a^* v_a^{*2}}{2(v_a^{*2} - a_a^{*2})}$$

$$A_3 = \frac{2k' a_a^{*2} A_2 + v_a^* \left[8(1+\Gamma) A_2^2 + 4(1+3\Gamma) u_a^* A_2 + (v_a^{*2} - a_a^{*2}) \right]}{6(v_a^{*2} - a_a^{*2})}$$

$$+ v_a^* \frac{\left[4\Gamma u_a^{*2} - 2k'\Gamma v_a^* (u_a^* + 2A_2) + k'^2 a_a^{*2} \right]}{6(v_a^{*2} - a_a^{*2})}$$

where

$$k' = \cot \varphi_a .$$

The corresponding v^* component is found by means of Eq. (2).

REFERENCES

1. Gross, R. A. and Oppenheim, A. K.: Recent Advances in Gaseous Detonation, ARS Jour., Vol. 29, No. 3, March 1959, pp 173-179.

2. Evans, Marjorie and Ablow, C. M.: Theories of Detonation. Jour. of Chemical Reviews, Vol. 61, No. 2, April 1961, pp 129-177.

3. Fletcher, E. A. Dorsch, R. G., and Allen, Harrison Jr.: Combustion of Highly Reactive Fuels in Supersonic Airstreams. ARS Jour., Vol. 30, No. 4, April 1960, pp 337-344.

4. Zeldovich, Ya. B. and Shlyapiutok, I. Ya.: Ignition of Explosive Gaseous Mixtures in Shock Waves (Translated from Doklady Akademii Nauk SSSR, Vol. LXV, No. 6, 1949, Moscow, pp 871-874). U.S. Dept. of Commerce OTS:60-41, 533, JPRS: 5781, Oct. 7, 1960.

5. Ruegg, Filmer W. and Dorsey, William W.: A Missile Technique for the Study of Detonation Waves, Jour. of Research of the National Bureau of Standards - C. Engineering and Instrumentation, Vol. 66C, No. 1, Jan.-Mar. 1962.

6. Gross, Robert A. and Chinitz, Wallace: A Study of Supersonic Combustion. Jour. Aero/Space Sciences, Vol. 27, No. 7, July 1960, pp 517-524.

7. Kydd, P. H. and Mullaney, G. J.: Supersonic Combustion. Combustion and Flame, Vol. 5, No. 4, Dec. 1961, pp 315-318.

8. Nicholls, J. A.: Stabilized Gaseous Detonation Waves. ARS Jour., Vol. 29, No. 1, Jan. 1959, pp 63-64.

9. Dugger, G. L.: Comparison of Hypersonic Ramjet Engines with Subsonic and Supersonic Combustion. Part II, Performance and Applications, Combustion and Propulsion, Fourth AGARD Colloquium, High Mach Number Air-Breathing Engines, Jaumotte, A. L. Lefebvre, A. H. and Rothrock, A. M., Editors, Pergamon Press, 1951, pp 84-119.

10. McLafferty, George H.: Relative Thermodynamic Efficiency of Supersonic Combustion and Subsonic Combustion Hypersonic Ramjets. ARS Jour., Vol. 30, No. 11, Nov. 1960, pp 1019-1021.

11. Weber, R. J. and Mackay, J. S.: An Analysis of Ramjet Engines Using Supersonic Combustion. NACA TN 4386, 1958.

12. Dunlap, R., Brehm, R. L., and Nicholls, J. A.: A Preliminary Study of the Application of Steady-State Detonative Combustion to a Reaction Engine. Jet Propulsion, Vol. 28, No. 7, July 1958, pp 451-456.

13. Larisch, E.: The Ramjet with Standing Detonation Wave. Paper presented at the Meeting of the Rumanian Academy, Timisoara, 1958.

14. Luidens, Roger W. and Flaherty, Richard J.: Analysis and Evaluation of Supersonic Underwing Heat Addition, NASA Memorandum 3-17-59E, April 1959.

15. Townend, L. H.: Effects of External Heat Addition on Supersonic Cruise Performance. The Aeronautical Quarterly, Vol. XII, Pt. 3, Aug. 1962, pp 203-211.

16. Kvashnina, S. S. and Chernyi, G. G.: Steady State Flow of Detonating Gas Around a Cone. PMM-Jour. of Applied Mathematics and Mechanics (Translation of Soviet Jour. PMM), Vol. 23, No. 1, 1959, pp 252-259.

17. Courant, R. and Friedricks, K. O.: Supersonic Flow and Shock Waves. Interscience, 1948, pp 406-415.

18. Seistrunk, R., Fabri, J., and Le Grives, E.: Some Properties of Stationary Detonation Waves. Fourth Symposium on Combustion, The Williams & Wilkins Co., Baltimore, 1953, pp 498-501.

19. Willmarth, W. W.: The Production of Aerodynamic Forces by Heat Addition on External Surfaces of Aircraft. The Rand Corp. RM-2078, Dec. 1957.

20. Woolard, Henry W.: Tables of Properties of Some Oblique Deflagrations in Supersonic Flow, The Johns Hopkins University Applied Physics Laboratory, TG-382, Sept. 1960.

21. Rutkowski, J. and Nicholls, J. A.: Considerations for the Attainment of a Standing Detonation Wave. Proc. of the Gas Dynamics Symposium on Aerothermochemistry, Northwestern University, Aug. 1955, pp 243-253.

22. Chinitz, W., Bohrer, L. C., and Foreman, K. M.: Properties of Oblique Detonation Waves. Fairchild Engine Division, Deer Park, N. Y., AFOSR RN 59-462 (ASTIA AD 215-267), April 15, 1959.

23. Tsien, Hsue-Shen: The "Limiting Line" in Mixed Subsonic and Supersonic Flow of Compressible Fluids. NACA TN 961, Nov. 1944.

24. Reyn, J. W.: Differential-Geometric Considerations on the Hodograph Transformation for Irrotational Conical Flow. Archives for Rational Mechanics and Analysis, Vol. 6, No. 4, 1960.

25. Staff of the Computing Section, Center of Analysis (Under Direction of Zdenek Kopal): Tables of Supersonic Flow of Air Around Cones. Technical Report No. 1, Mass. Inst. Tech., 1947.

26. Fettis, Henry E.: An Approximate Solution to Supersonic Conical Flow. Jour. Aero. Sciences, Vol. 23, No. 12, Dec. 1956, pp 1122-1123.

27. Hord, Richard A.: An Approximate Solution for Axially Symmetric Flow Over a Cone with an Attached Shock Wave. NACA TN 3485, Oct. 1955.

28. Hammitt, A. G. and Murthy, K. R. A.: Approximate Solutions for Supersonic Flow Over Wedges and Cones. Dept. of Aeronautical Engineering, Princeton Univ. Rept. No. 449, (AFOSR TN 59-304, AD 213 088), April 1958. Also Jour. Aerospace Sciences, Vol. 27, No. 1, Jan. 1960, p 71.

29. Zienkiewicz, H. K.: Flow About Cones at Very High Speeds. The Aeronautical Quarterly, Vol. 8, Pt. 4, Nov. 1957, pp 384-394.

30. Pottsepp, L.: Inviscid Hypersonic Flow Over Unyawed Circular Cylinders. Jour. Aerospace Sciences, Vol. 27, No. 7, July 1960, pp 558-559.

31. Powers, S. A.: Comment on "Inviscid Hypersonic Flow Over Unyawed Circular Cones". Journal of the Aerospace Sciences, Vol. 28, No. 2, Feb. 1961, pp 163-164.

32. Ames Research Staff: Equations, Tables and Charts for Compressible Flow. NACA Report 1135, 1953.

33. Kennedy, E. C. and Kerr, H. C.: Tables of Supersonic Conical Flow. Convair Ordnance Aerophysics Laboratory OAL Memorandum 143, OAL/CM-973, May 16, 1960.

TABLE I

Numerical Values of the Omega Functions
for Several Specific-Heat Ratios[a]

	$\gamma = 1.2$	$\gamma = 1.3$	$\gamma = 1.4$	$\gamma = 1.405$
Ω_1	1.5732	1.6086	1.6432	1.6449
Ω_2	-0.45455	-0.47101	-0.48611	-0.48683
Ω_3	-0.045455	-0.028986	-0.013889	-0.013167
Ω_4	0.049219	0.043912	0.039403	0.039196
Ω_5	0.13480	0.12726	0.12027	0.11993
Ω_6	-0.18402	-0.17117	-0.15967	-0.15913
Ω_7	-0.0056692	-0.0060097	-0.0062160	-0.0062234
Ω_8	-0.063259	-0.060677	-0.058299	-0.058185
Ω_9	0.0045413	0.0046842	0.0043877	0.0043640
Ω_{10}	0.018314	0.016616	0.015874	0.015857
Ω_{11}	-0.017186	-0.015290	-0.014046	-0.013997

[a]See Appendix C for omega function relations.

TABLE II

Comparison of Approximate and Exact Calculations

EXAMPLE NO.	φ_s (Deg)	u_s^*	φ_T (Deg)	φ_B (approx) (Deg)	φ'_B (exact, Kopal) (Deg)	u_B^* (approx)	$u_B^{*'}$ (exact, Kopal)	$\frac{\varphi_s - \varphi'_B}{\varphi_s}$	$\frac{\varphi_B - \varphi'_B}{\varphi'_B}$	$\frac{u_B^* - u_B^{*'}}{u_B^{*'}}$	M_{O_J}
I	68.556	0.30969	54.62	39.65	40	0.40050	0.40	0.416	-0.009	0.0013	N.S.[a]
II	62.732	0.29072	47.89	29.61	30	0.40083	0.40	0.521	-0.013	0.0021	2.168
III	52.347	0.43227	41.12	29.87	30	0.50049	0.50	0.427	-0.004	0.0010	2.948
IV	45.997	0.55665	37.29	29.97	30	0.60015	0.60	0.348	-0.001	0.0003	10.48
V	69.385	0.15519	43.67	9.22	10	0.40190	0.40	0.855	-0.078	0.0048	1.091
VI	46.587	0.36690	28.39	9.34	10	0.50180	0.50	0.783	-0.066	0.0036	1.403
VII	20.947	0.77562	13.81	9.85	10	0.80022	0.80	0.523	-0.015	0.0003	3.360

[a]No solution exists.

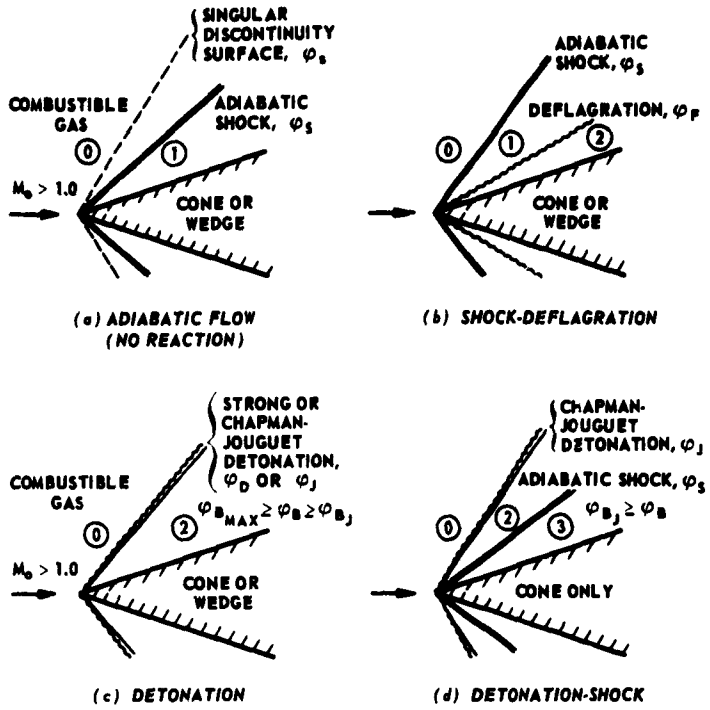

Fig. 1 CONICAL FLOW REGIMES FOR INSTANTANEOUS CHEMICAL REACTION

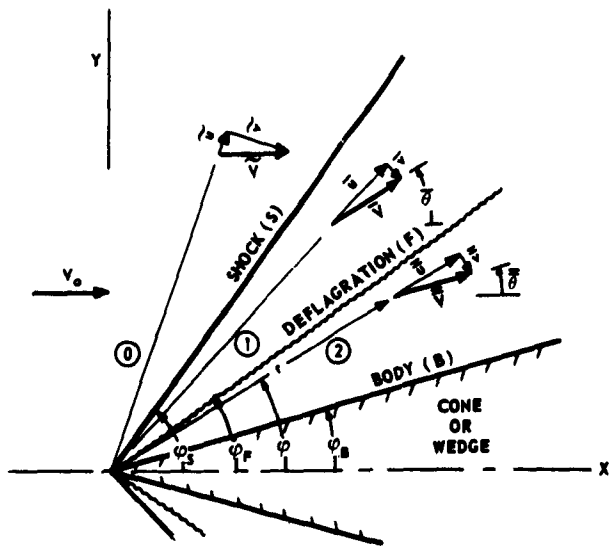

Fig. 2 ILLUSTRATION OF NOTATION

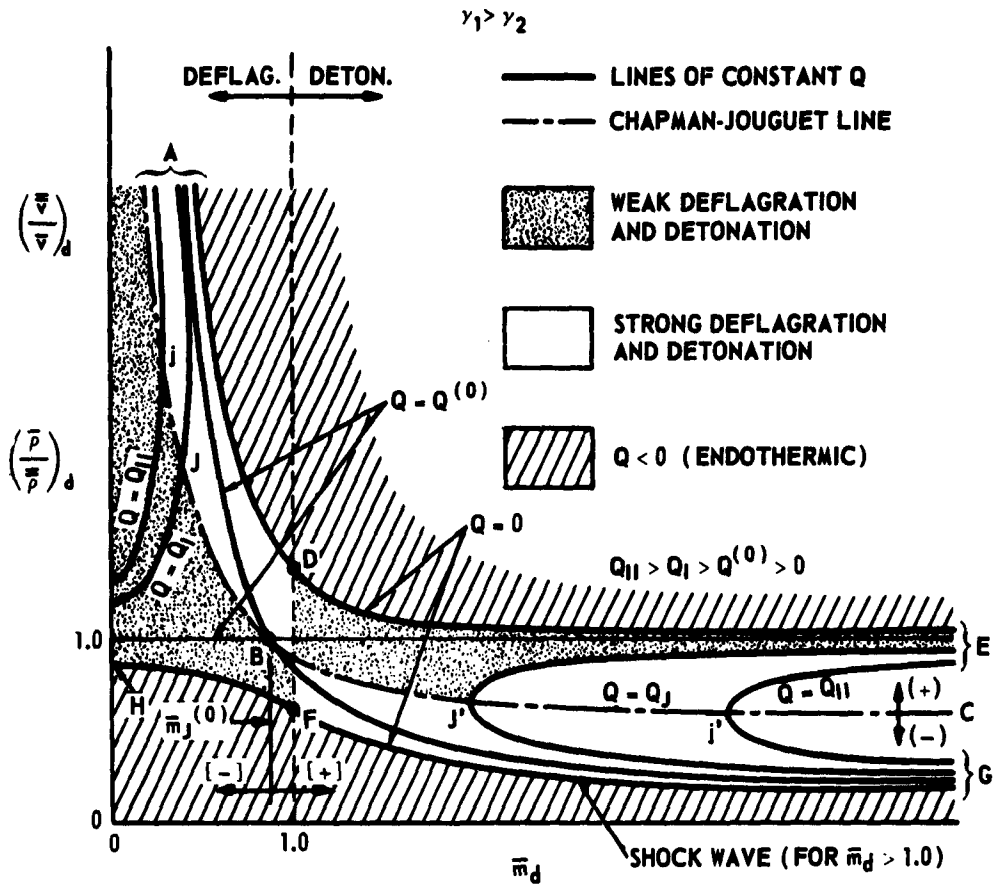

Fig. 3 SCHEMATIC ILLUSTRATION OF NORMAL-FLOW REGIMES FOR OBLIQUE EXOTHERMIC DISCONTINUITIES

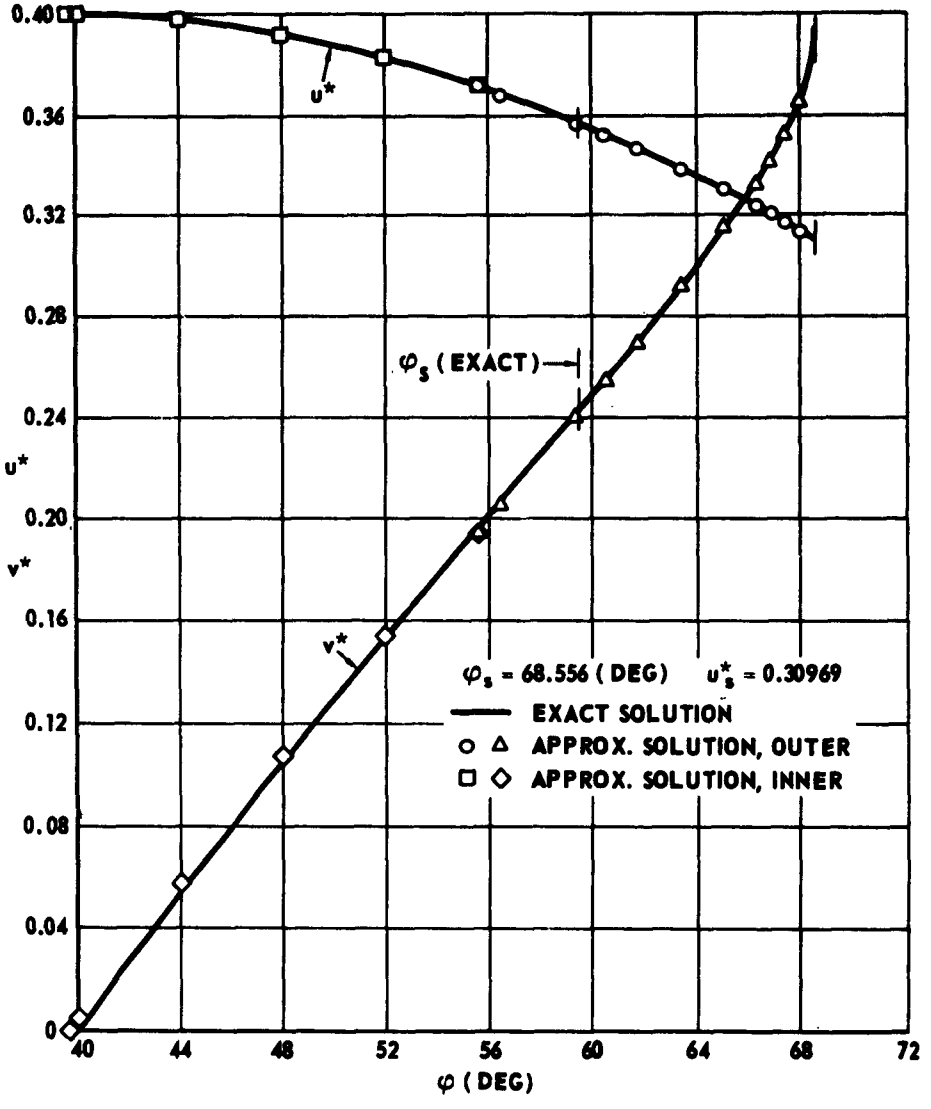

Fig. 5 COMPARISON OF EXACT AND APPROXIMATE CONE FLOW FIELDS

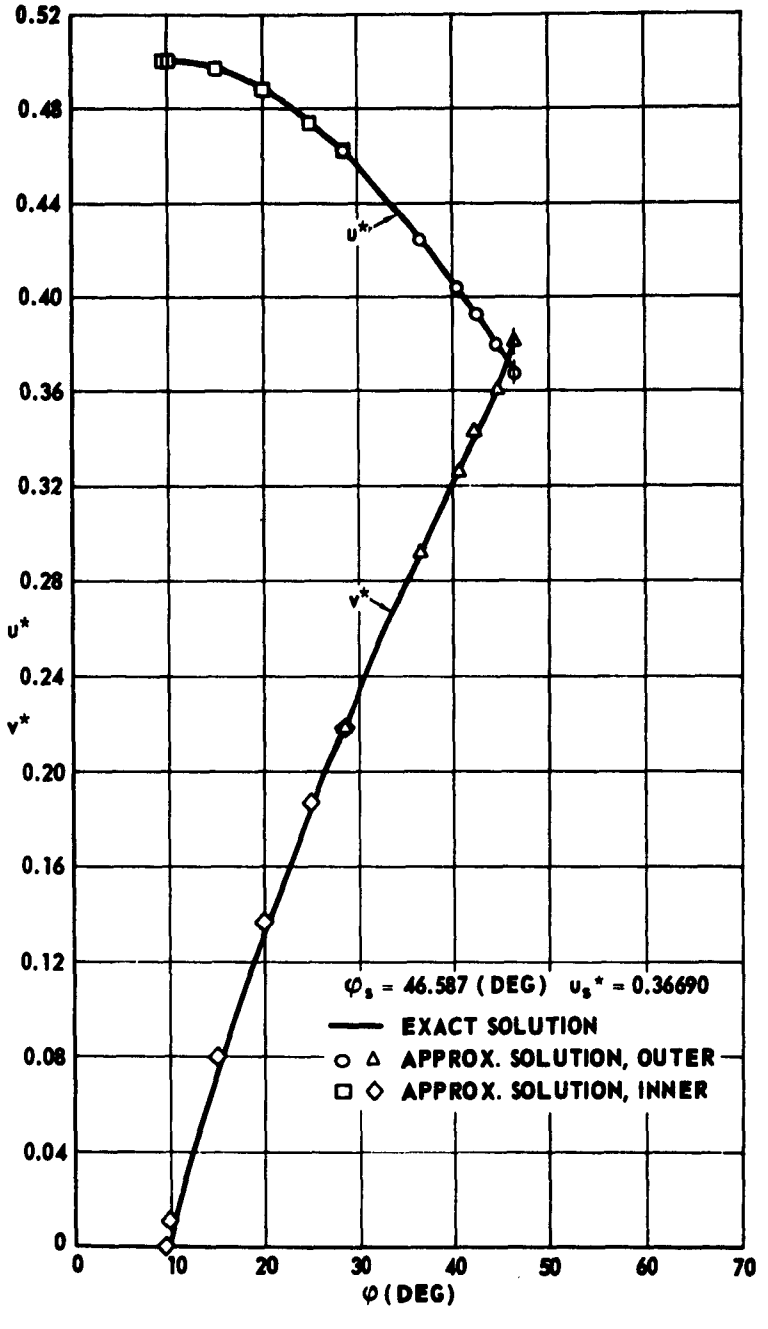

Fig. 6 COMPARISON OF EXACT AND APPROXIMATE CONE FLOW FIELDS

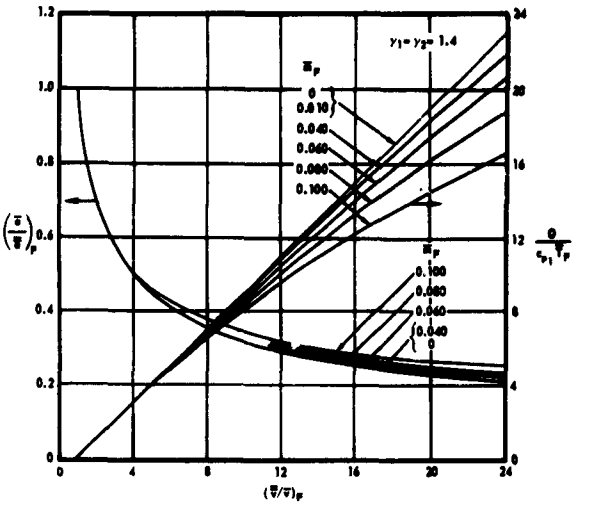

Fig. 7 SOME PROPERTIES OF OBLIQUE DEFLAGRATIONS

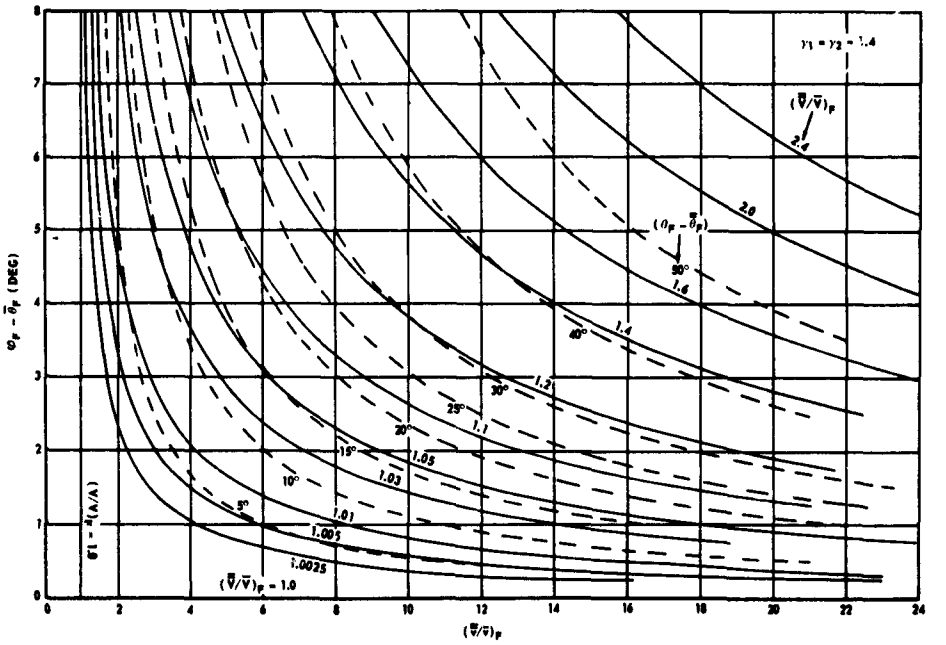

Fig. 8 SOME PROPERTIES OF OBLIQUE DEFLAGRATIONS

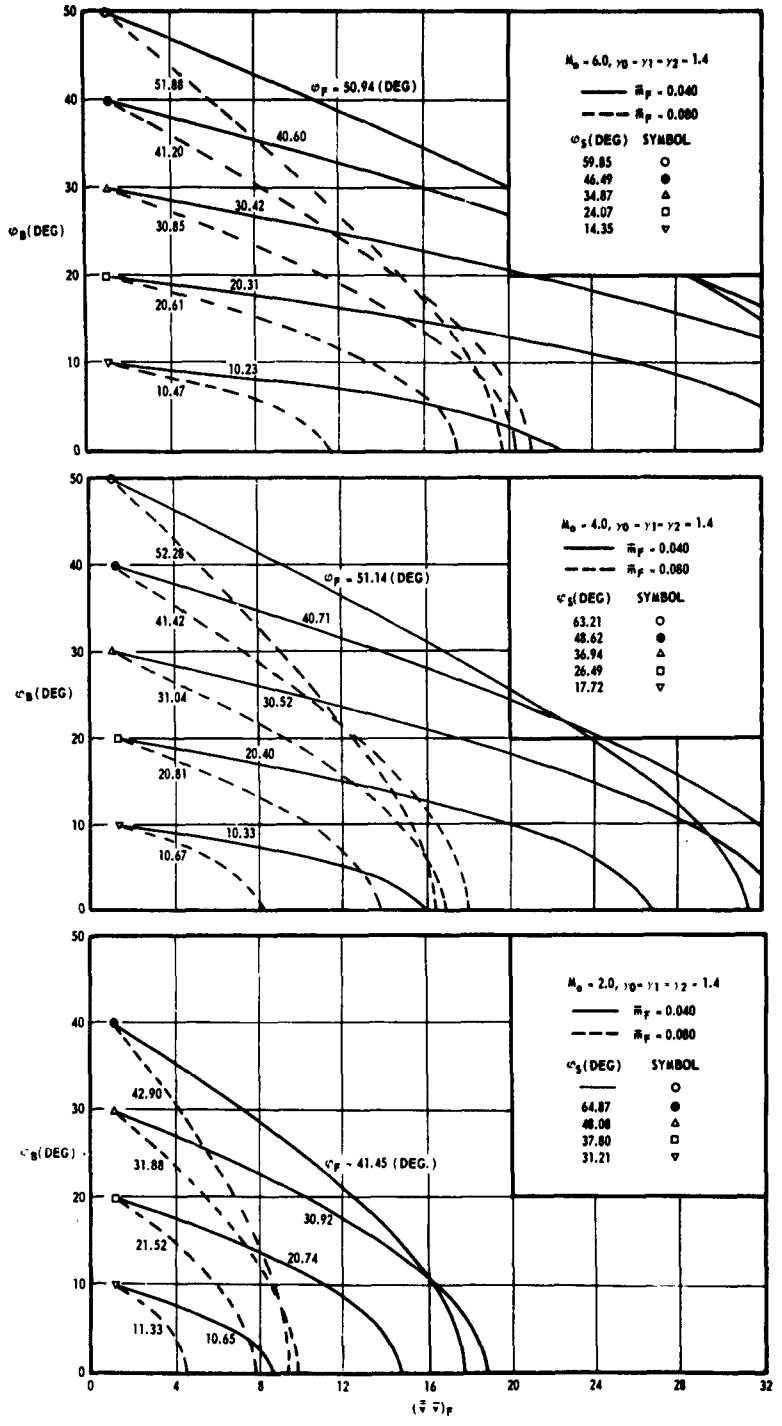

Fig. 9 SOME PROPERTIES OF SHOCK-DEFLAGRATIONS FLOWS FOR CONES

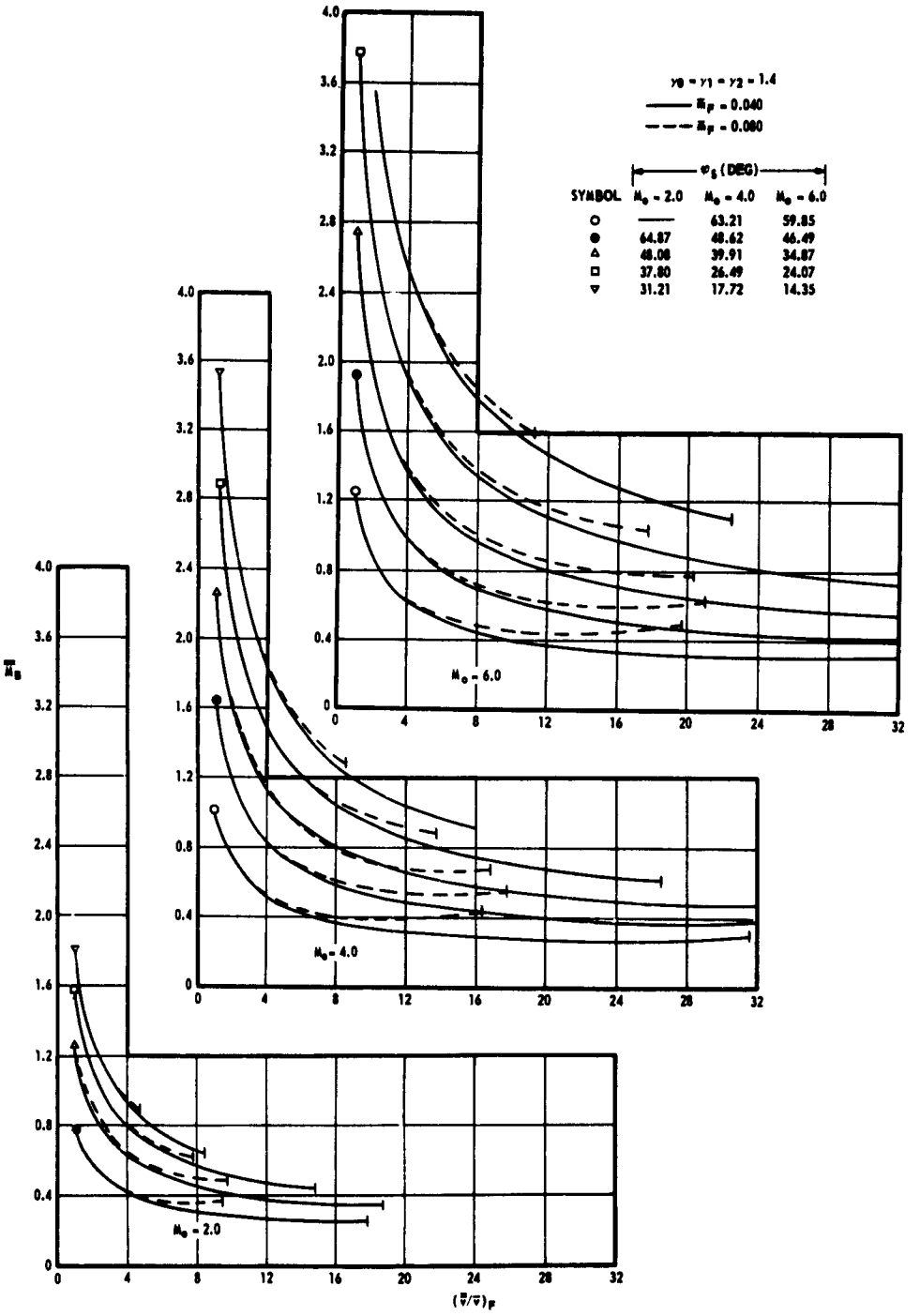

Fig. 10 CONE-SURFACE MACH NUMBER FOR SHOCK-DEFLAGRATION FLOWS

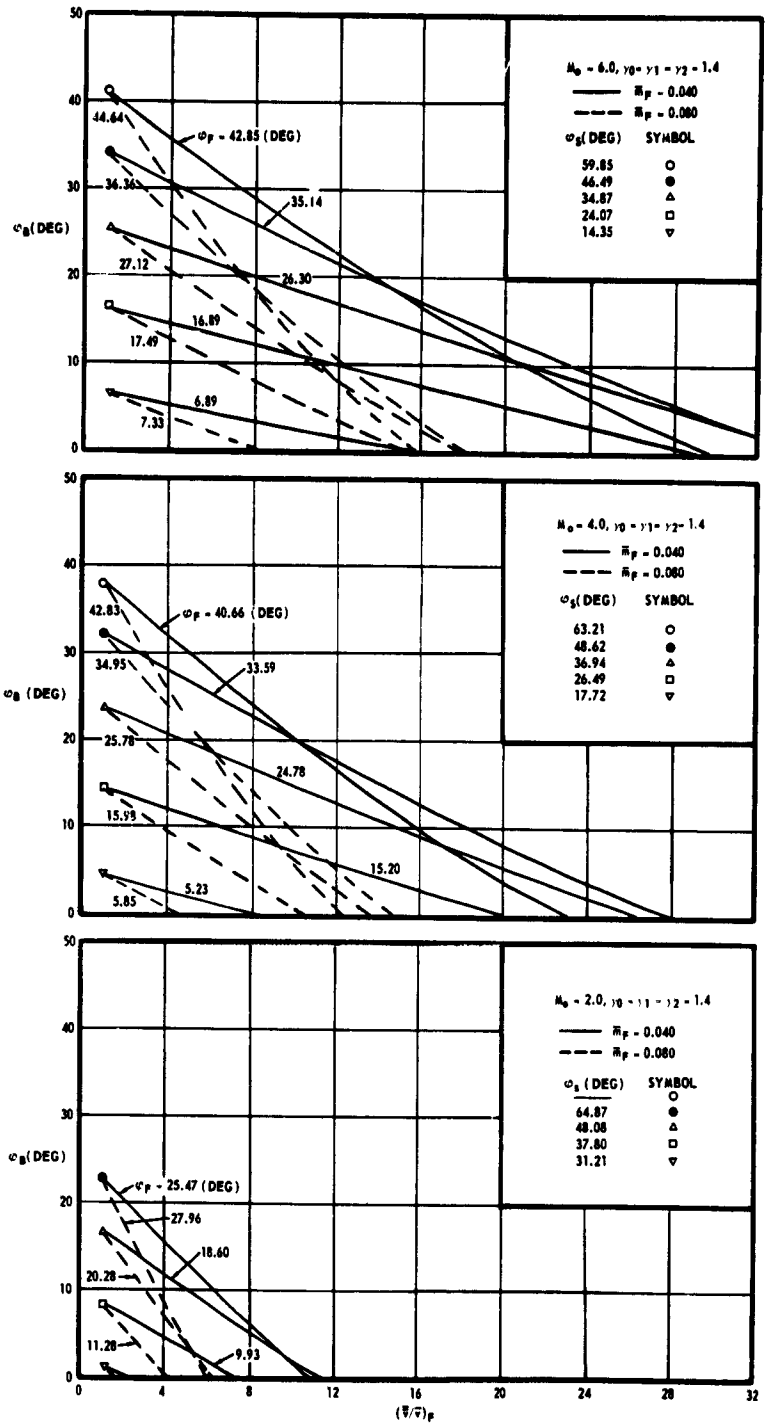

Fig. 11 SOME PROPERTIES OF SHOCK-DEFLAGRATION FLOWS FOR WEDGES

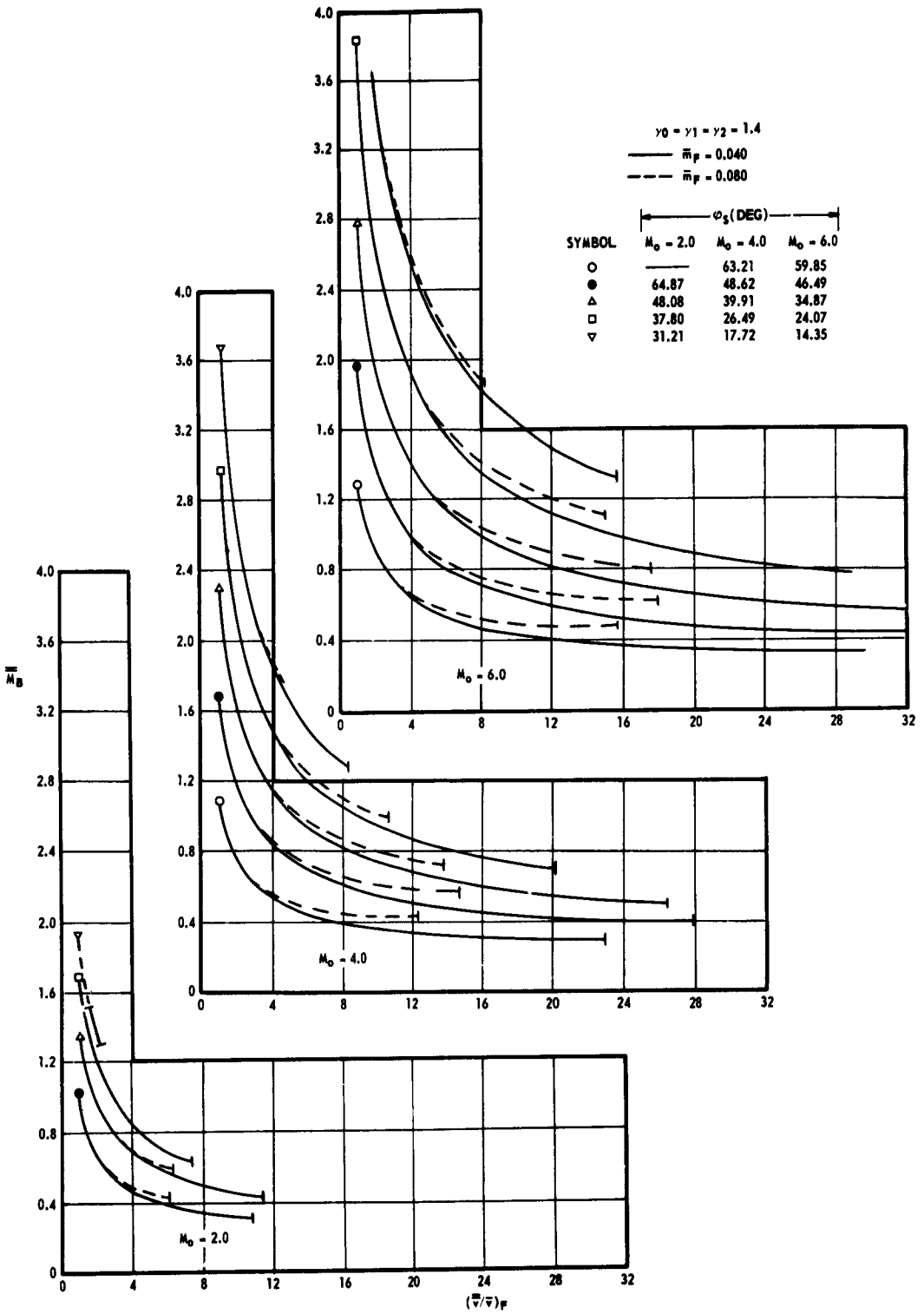

Fig. 12 WEDGE-SURFACE MACH NUMBER FOR SHOCK-DEFLAGRATION FLOWS

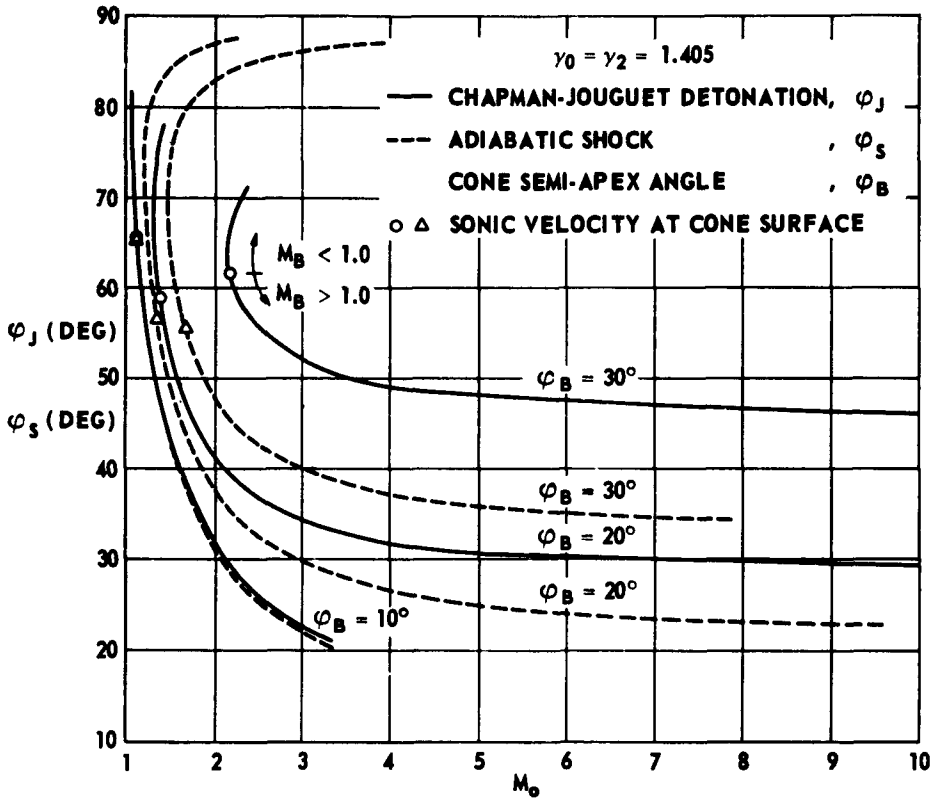

Fig. 13 WAVE ANGLES OF CHAPMAN-JOUGUET DETONATIONS AND ADIABATIC SHOCKS FOR CONE FLOW

The Johns Hopkins University
APPLIED PHYSICS LABORATORY
Silver Spring, Maryland

Initial distribution of this document has been made in accordance with a list on file in the Technical Reports Group of the Applied Physics Laboratory, The Johns Hopkins University.